nature reviews clean technology

https://doi.org/10.1038/s44359-026-00184-z

Review article

Check for updates

Hydrogen-based materials for energy storage and conversion

Darren P. Broom[1], Mark D. Allendorf[2,3], Tom Autrey[4], Marcello Baricco[5], Jose Bellosta von Colbe[6], Mark E. Bowden[4], Craig E. Buckley[7], Ping Chen[8], Fermin Cuevas[9], Stefano Deledda[10], Martin Dornheim[11], Michael Felderhoff[12], Vanessa Fierro[13], Yaroslav Filinchuk[14], David M. Grant[11], Bjørn C. Hauback[10], Terry D. Humphries[7], Jacques Huot[15], Craig M. Jensen[16], Torben R. Jensen[17], Peter Ngene[18], Hyunchul Oh[19], Shin-ichi Orimo[20,21], Luca Pasquini[22], Kouji Sakaki[23], Sabrina Sartori[24], Godwin Severa[25], Colin J. Webb[26], Claudia Weidenthaler[12], Brandon C. Wood[27], Volodymyr A. Yartys[10,28], Min Zhu[29] & Michael Hirscher[20,30]

Abstract

Hydrogen has the highest gravimetric energy density of any energy carrier and it can operate in a closed cycle with no carbon emissions. Hydrogen-based materials play a critical part in hydrogen storage and helped to power the first generation of hybrid electric vehicles. In this Review, we examine several clean-energy applications of hydrogen-based materials. A major focus of research is hydrogen storage and transportation. Storing hydrogen gas is challenging, but physisorption by nanoporous materials, absorption by metal and complex hydrides, and liquid hydrogen carriers offer viable solutions for safe and economical hydrogen storage. For many applications in a future hydrogen economy, hydrogen gas must be compressed and metal hydride compressors can achieve the pressures required by the type IV compressed-gas storage tanks used in the first generation of commercial fuel cell vehicles. Hydrides are still relevant for battery technology, including as electrodes in the next generation of nickel-metal hydride batteries, as electrolytes in future solid-state batteries, or as liquid electrolytes in new battery types. Hydrides also show promise as thermal energy storage materials for the utilization of industrial waste heat and for renewable energy sources such as solar thermal power plants. We review the status of each of these technologies, which are at varying stages of implementation, providing a basis for future research on hydrogen-based materials for energy storage and conversion.

Sections

A full list of affiliations appears at the end of the paper. e-mail: m.hirscher@fkf.mpg.de

Key points

- Short-term, highly reversible hydrogen storage can be achieved by physisorption of molecular hydrogen on high-surface-area porous materials.
- Metal hydrides can be used in high-density, long-term hydrogen storage at near-ambient pressure and temperature.
- Liquid organic hydrogen carriers and ammonia are widely considered as possible, safe hydrogen carriers for long-distance transport and large-scale hydrogen storage.
- Metal-hydride-based compressors can reach the high pressures required for type IV tanks without needing the moving parts of conventional mechanical compressors.
- Metal hydrides are the basis of a range of batteries, from the nickel-metal hydride batteries still in widespread commercial use through to novel solid- and liquid-state magnesium and calcium batteries.
- Compared with current thermal energy storage technologies, metal hydrides have high heat storage capacities and can reduce the system size for heat storage in concentrated solar plants or for waste heat utilization.

Introduction

Effective use of hydrogen-based materials and liquid hydrogen carriers could accelerate the transition to a zero-emission society[1]. Increased use of renewable energy sources, such as wind and solar, demands the development of cost-efficient energy storage technologies and energy carriers. Hydrogen-based materials play an important part in such applications, including hydrogen storage and transportation, hydrogen processing (as in efficient hydrogen compressors and hydrogen purification) as well as thermal energy storage and electrochemical energy storage in batteries. Furthermore, hydrogen-based materials have the advantage of being multifunctional, making them useful for isotope separation, as superconductors, catalysts, sensors and so forth[2] (Fig. 1).

Hydrogen can bind to materials by forming either physical or chemical bonds[3]. In nanoporous materials, such as metal–organic frameworks (MOFs) and nanoporous carbons, hydrogen molecules interact physically with surfaces via weak van der Waals forces. Cryogenic temperatures, typically 77 K, are therefore required for hydrogen storage, and a large amount of hydrogen adsorption requires a high accessible surface area[4]. In metal hydrides, H_2 molecules dissociate into H atoms on the surface and absorb into the bulk of the material. Chemical bonds between the H atoms and surrounding elements are formed that can be ionic, covalent or metallic. Intermediate types can occur as well, such as MgH_2, with mixed ionic and covalent bonding. Metallic hydrides comprise a wide variety of stoichiometric and non-stoichiometric compounds in which H acts as a metal and occupies interstitial positions between the host metal atoms in the crystal structure[5]. Complex hydrides are salts with hydrogen-containing anions or a hydride anion. They usually contain more than one type of bond, for example, both ionic and covalent, and more than one type of metal or metal cation[6–8]. Formation of a metal or complex hydride is typically an exothermic process: releasing energy while absorbing hydrogen and requiring the addition of heat or energy to subsequently release hydrogen.

Among liquid-state hydrogen carriers, liquid organic hydrogen carriers (LOHCs) — including hydrocarbons, alcohols and aqueous formate solutions — and ammonia (NH_3) are the most promising for hydrogen storage and transport[9]. In contrast to liquid hydrogen, which requires cryogenic temperatures below 30 K, LOHCs can be stored under ambient conditions and the hydrogen sorption process occurs via a catalytic reaction. Ammonia contains 17.6 wt% hydrogen and is therefore an attractive hydrogen carrier, in particular for long-distance transportation.

Research into hydrogen-based materials for energy storage and conversion continues to develop. For hydrogen storage and transportation, advances in balancing the volumetric and gravimetric capacities of MOFs have been reported[10]; scaled-up metal hydride stores, incorporating thermal management systems, have been developed[11]; and new low-enthalpy LOHCs have been investigated[12], together with novel ammonia synthesis and decomposition approaches[13,14]. The use of metal hydrides for hydrogen compression has seen advances in the modelling of metal hydride compressors[15,16] and the development of systems suitable for compression to pressures >700 bar[17,18]. New complex hydride-based electrolytes for solid-state batteries (SSBs) have been reported[19] and hydride-based heat storage systems have been developed to demonstrate the practical utility of metal hydrides for thermal energy storage[20].

In this Review, we discuss different classes of hydrogen-based materials and their applications in clean technology. The main focus will be on hydrogen storage and transportation, for which three different classes of materials are considered: nanoporous materials, metal and complex hydrides, and liquid hydrogen carriers. We will then discuss hydrogen compression, before covering electrochemical energy storage both in nickel-metal hydride batteries and in batteries using complex hydrides as solid and liquid electrolytes. Finally, thermal energy storage using metal hydrides for waste heat utilization and for renewable energy sources such as solar plants will be discussed.

Hydrogen storage and transportation

Hydrogen can be stored and transported as a gas, pure liquid or physically or chemically bound in materials[3,21,22]. Compressed-gas storage at high pressure (up to 700 bar) and liquefied hydrogen at low temperatures (below 30 K) are mature technologies, but both methods have disadvantages. Compression consumes energy and high-pressure (type IV) tanks are expensive, while liquefaction consumes up to 35% of the energy stored in the hydrogen, requires costly insulated tanks and suffers boil-off losses over time[23]. Nevertheless, these storage methods are used for mobile applications, as well as for large-scale hydrogen storage[24]. Type IV tanks are currently used in commercial hydrogen fuel cell vehicles, providing gravimetric and volumetric system capacities of around 5.7 wt% and 40 g l^{-1}, respectively. Liquid hydrogen has a volumetric hydrogen density of 70.8 g l^{-1}, but liquid vessels tested in heavy-duty trucks have system storage capacities of 8.7 wt% and 43.3 g l^{-1} (ref. 25). These storage capacities, on a system basis, provide valuable benchmarks for alternative hydrogen storage in solids or liquids. Materials are typically characterized by gravimetric density and volumetric density on a materials basis. When included in a system with containment, heat management and insulation, both volumetric and gravimetric system capacities are reduced compared with the material density, but in some cases, volumetric

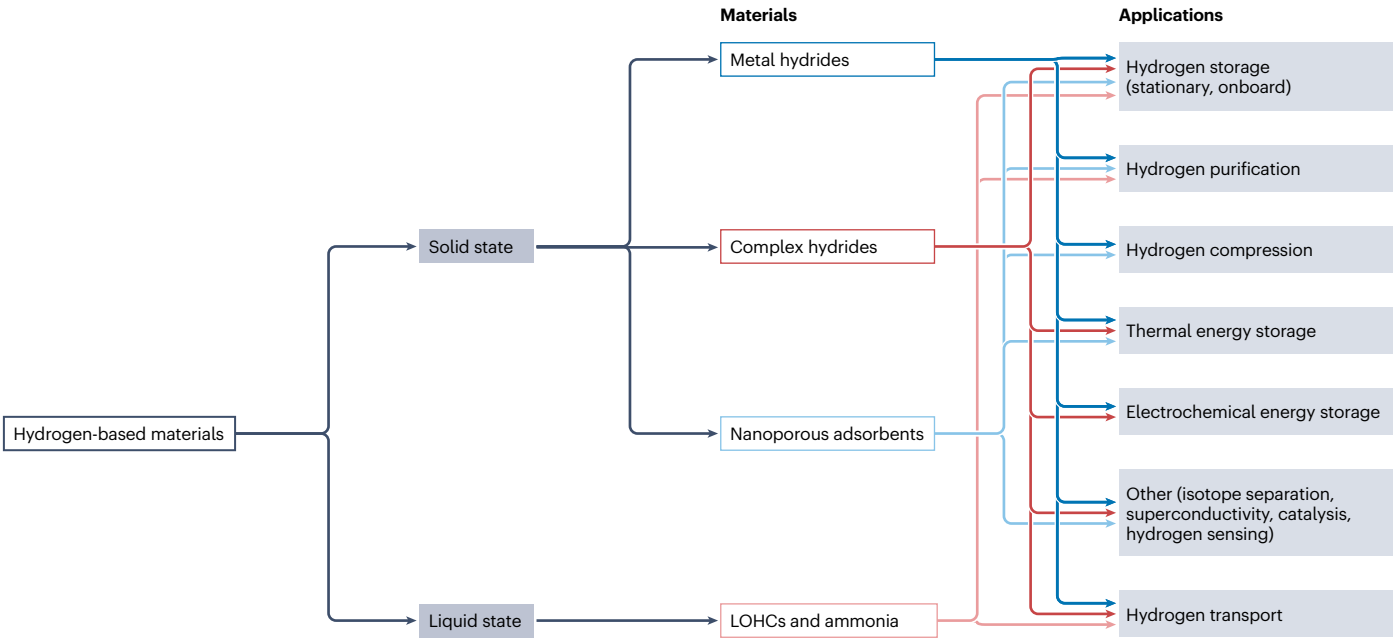

Fig. 1 | Overview of hydrogen-based materials and their applications. Hydrogen-based materials can be in a solid or liquid state. Liquid-state materials discussed here include liquid organic hydrogen carriers (LOHCs) and ammonia. Solid-state materials are metal hydrides, complex hydrides and nanoporous adsorbents, each of which exhibit different chemical and physical interactions with hydrogen. Each material type has multiple applications.

capacity can nearly be maintained since only low-pressure vessels are required[26]. In this section, storage capacities will be given on a materials basis, bearing in mind the above benchmarks for storage systems.

Physisorption by nanoporous materials

Nanoporous materials store hydrogen by physically adsorbing molecular hydrogen on their large internal surfaces, mainly through van der Waals interactions. This adsorption process is known as physisorption and results in a higher density of hydrogen in the pore network, compared with the bulk gas density at the same temperature and pressure. Physical interactions of hydrogen with surfaces are generally weak, so a large amount of adsorption requires low temperatures, around 77 K (Fig. 2). Nanoporous materials include activated carbons and MOFs[27]. Activated carbons have been used industrially for over a century[28]. They are formed by physically or chemically activating organic precursors, to create highly porous materials, with large surface areas and distributions in pore size owing to their amorphous or microcrystalline structure. Activated carbons have been considered for hydrogen storage since the 1970s[29]. MOFs, meanwhile, are highly ordered materials synthesized by combining metal ions or clusters with organic linkers to form extended crystalline porous networks. Hydrogen storage in MOFs was first reported over 20 years ago and has been studied extensively since[27]. Other nanoporous materials include zeolites, microporous organic polymers, and various types of nanoporous carbon, such as carbide-derived carbons, zeolite-templated carbons and aerogels, all of which have been considered for hydrogen storage.

The performance of these materials depends strongly on their porous properties – including specific surface area (SSA), pore size and total pore volume – as well as the chemistry of the material. Gravimetric hydrogen uptakes scale approximately with SSA (Fig. 2b), as determined using the Brunauer–Emmett–Teller method with nitrogen (N_2) or argon adsorption isotherms at 77 or 87 K, respectively. All types of nanoporous material have a range of SSAs – activated carbons from just a few hundred$m^2\,g^{-1}$ to approximately 3,300 $m^2\,g^{-1}$, with some MOFs exceeding 5,000 $m^2\,g^{-1}$ (ref. 4). An early focus of MOF research was to discover new materials with ever higher SSAs[30]. For hydrogen storage, this research led to increased gravimetric capacities, exceeding 10 wt% in some materials with very high SSAs[30]. Materials with high SSAs, however, have open structures, leading to poor volumetric capacities, which results in a trade-off between gravimetric and volumetric capacity[31].

Early studies of MOFs[32] and other nanoporous materials, including novel carbons[33], also tended to report maximum uptake, either the excess adsorbed quantity or absolute adsorbed quantity measured at elevated pressure. For practical applications, however, the usable capacity is more important. Usable capacity is the reversible capacity between the maximum storage pressure and delivery pressure, typically a few bar, and it defines the amount of hydrogen that can be delivered from a store[34,35]. Both pressure and temperature swings can be considered[36]. The relationship between the properties of a material and usable capacity is complex, involving various factors such as SSA, pore volume, chemistry and the range of temperature and pressure in operation.

Balancing gravimetric and volumetric capacity remains a critical factor in optimizing storage performance[10,37,38]. Considerable effort has therefore focused on enhancing volumetric capacity while maintaining high gravimetric performance, with an emphasis on the importance of optimizing pore size and structure. In particular, compacting and shaping materials into monoliths has become central to increasing

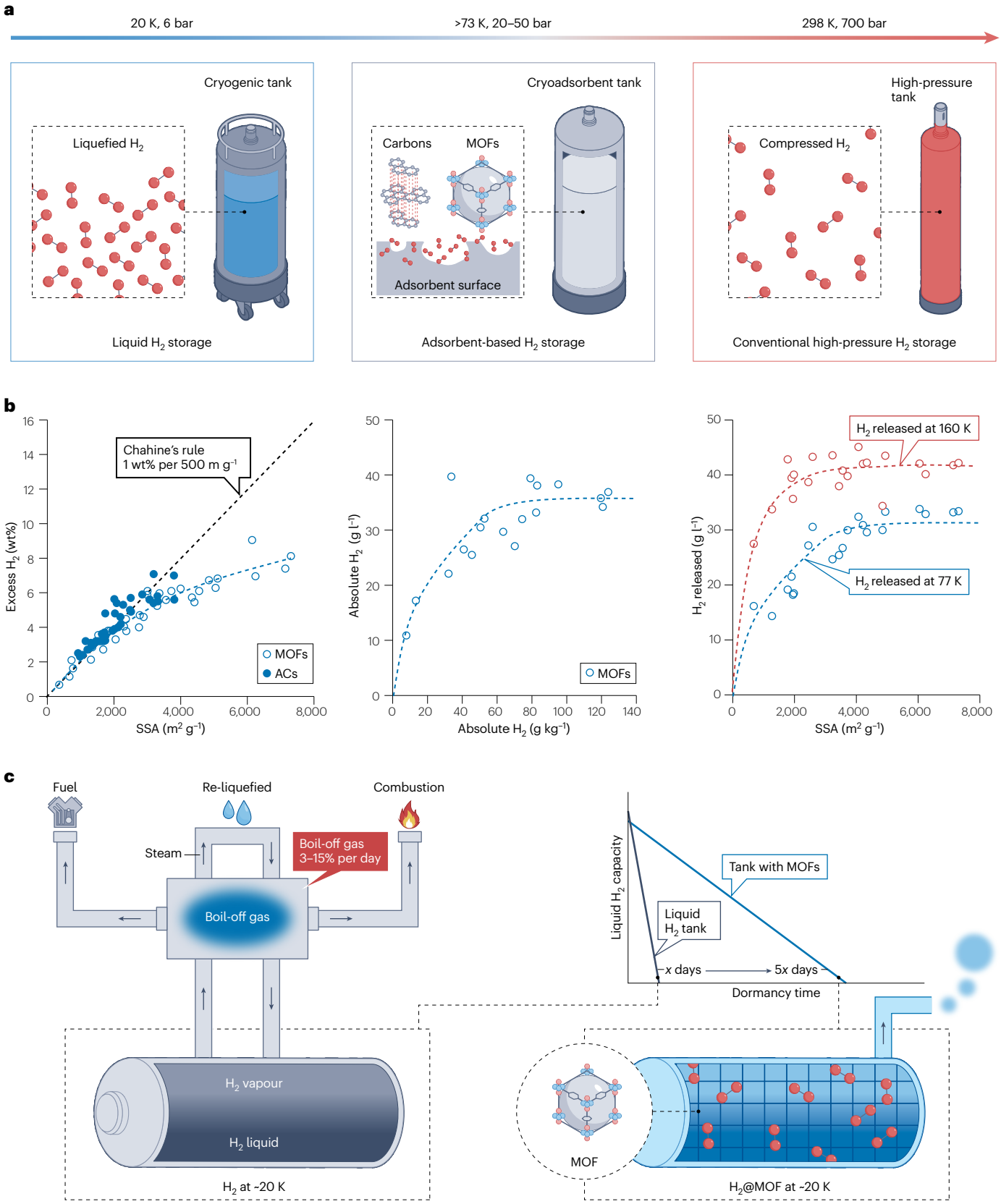
a
20 K, 6 bar
>73 K, 20–50 bar
298 K, 700 bar
Cryogenic tank
Liquefied H_2
Liquid H_2 storage
Cryoadsorbent tank
Carbons
MOFs
Adsorbent surface
Adsorbent-based H_2 storage
High-pressure tank
Compressed H_2
Conventional high-pressure H_2 storage
b
Chahine's rule
1 wt% per 500 m g^{-1}
Excess H_2 (wt%)
SSA (m^2 g^{-1})
MOFs
ACs
Absolute H_2 (g l^{-1})
Absolute H_2 (g kg^{-1})
MOFs
H_2 released at 160 K
H_2 released at 77 K
H_2 released (g l^{-1})
SSA (m^2 g^{-1})
c
Fuel
Re-liquefied
Combustion
Steam
Boil-off gas
3–15% per day
Boil-off gas
H_2 vapour
H_2 liquid
H_2 at ~20 K
Liquid H_2 capacity
Tank with MOFs
Liquid H_2 tank
x days
5x days
Dormancy time
MOF
H_2@MOF at ~20 K

Fig. 2 | Hydrogen storage in nanoporous materials. a, Cryogenic liquid hydrogen storage, adsorbent-based hydrogen storage using nanoporous materials, and conventional high-pressure hydrogen storage, with the pressure and temperature conditions required for each method shown. **b**, Left, gravimetric hydrogen adsorption at 77 K as a function of specific surface area (SSA) for metal–organic frameworks (MOFs, open circles) and activated carbons (ACs, filled circles). Centre, relationship between absolute hydrogen uptake on a gravimetric (g kg^{-1}) and volumetric (g l^{-1}) basis at 77 K, demonstrating the saturation behaviour of MOFs. Right, hydrogen release as a function of SSA at different temperatures (77 K and 160 K) for MOFs. Plotted data and their sources are tabulated in the Supplementary Information. **c**, Left, three established approaches to mitigating boil-off gas losses in liquid hydrogen storage. Right, a novel adsorption-based strategy for minimizing boil-off gas loss, using MOFs at cryogenic temperatures (~20 K)[58].

volumetric capacity[39,40]. This approach allows for denser packing of adsorbent materials, leading to more efficient use of space within storage tanks. However, achieving such advances requires careful control over pore size distribution to maximize hydrogen adsorption while preserving the structural integrity of the materials[41,42].

The advent of MOFs reinvigorated research into hydrogen storage in nanoporous materials, thanks to their very high SSAs and tunable porosity. A large number of different structures exist, and MOFs can also exhibit framework flexibility and possess open metal sites[43–45]. Framework flexibility can result in changes in isotherm shape, increasing usable capacity[37,46], while open metal sites interact more strongly with hydrogen and can increase operating temperature[43,45]. MOF structures can also interpenetrate, offering the possibility of increasing volumetric capacity by filling space more efficiently and providing small pores for stronger adsorption[47,48]. MOFs also consist mainly of light elements, thus maximizing gravimetric capacities.

Compared with compressed hydrogen, the presence of an adsorbent in a tank lowers the maximum required pressure for storing the same amount, making storage safer and reducing the energy required to compress hydrogen. The operating temperature (typically 77 K) is higher than the boiling point of liquid hydrogen, thus avoiding the energetic cost of liquefaction[4,40]. In comparison to hydrides, the adsorption process is also fully reversible and rapid, which is desirable in practical applications.

Materials development for hydrogen storage using physisorption has progressed, including optimized structures and high capacities, but scaling up and system integration are now required. Scaling up of porous materials can be difficult and challenging[49]; however, various companies have started to scale up MOF production[50]. The field is now moving towards the stage of demonstration tanks[4]. Despite the low heat of adsorption of hydrogen in most nanoporous materials (typically 4 to 7 kJ mol^{-1}), heat management is still an issue during rapid charging, requiring the inclusion of heat-transfer material in a tank, given that large temperature changes occur when hydrogen is introduced to a material bed. Room-temperature storage is the ideal, but no nanoporous material has so far been discovered that can adsorb hydrogen to a usable level under such conditions. Reproducibility issues have hindered progress on porous materials for hydrogen storage[51,52], but the proposal[53] to use a MOF (ZIF-8), in a pelletized form[54], as a reference material is a step towards standardization[55].

Physisorption-based hydrogen storage could also be well suited to long-distance transportation and applications requiring extended storage durations. Nanoporous materials, such as MOFs, can retain hydrogen at cryogenic temperatures, reducing the boil-off losses often seen in liquid hydrogen storage (Fig. 2c). Below 33 K, these materials allow hydrogen molecules to form super-dense layers on their internal surfaces, achieving storage densities that meet or exceed those of liquid hydrogen without requiring liquefaction[56,57]. This characteristic makes advanced cryo-adsorbents particularly effective for stable, long-term hydrogen storage and cross-continental transport, offering a practical solution to natural vaporization losses[58]. Such vaporization reduction in liquid hydrogen tanks was previously only possible using highly efficient insulation or re-liquefying devices[59]. However, the stronger interactions within nanoporous structures at 20 K mean that physisorption can enhance local sorption density, providing a promising approach to minimizing vaporization with storage capacity comparable to that of liquid hydrogen inside the storage tank.

Metal and complex hydrides

Metal and complex hydrides can store hydrogen in the solid state, with some able to operate at near-ambient temperatures and mild pressures, below 30 bar[7,60]. High volumetric capacities, up to around 120 g l^{-1} (nearly twice the density of liquid hydrogen) can be achieved using hydrides, but challenges include cost, reversible gravimetric capacity, the kinetics and operating temperatures.

Intermetallic compounds of interest for hydrogen storage include the compositions AB, AB_2 and AB_5, where A and B are typically elements with high and low H affinities, respectively[61–63]. TiFe (ref. 64), $ZrMn_2$ (ref. 65) and $LaNi_5$ (refs. 66,67) are examples. These compounds form hydrides by hosting H in the interstitial sites of the crystal lattice. Thousands of alloys with partial elemental substitutions on the A and B sites have been investigated (as in the HyMarc Data Hub), including sub- and super-stoichiometric compositions. In addition, medium-entropy alloys with three or four elements of a similar concentration[68] and high-entropy alloys consisting of five or more elements[69,70] have been explored as potential hydrogen storage materials. Examples of high-entropy alloys include TiVZrNbHf[71] and $Mg_{0.1}Ti_{0.3}V_{0.25}Zr_{0.1}Nb_{0.2}$ (ref. 72). Complex hydrides, by contrast, consist of an anion with H covalently bound to a central atom, such as $[BH_4]^-$ or $[AlH_4]^-$, which forms an ionic solid with an alkaline or alkaline-earth cation. Examples include $LiBH_4$, $NaAlH_4$, $Mg(BH_4)_2$ and Mg_2NiH_4 (refs. 7,8,73).

Intermetallic hydrides typically have modest gravimetric storage capacities in the range 1–2 wt%. They have moderate decomposition enthalpies ΔH, in the range 25–35 kJ mol^{-1}, resulting in hydrogen release at 1 bar at near-ambient temperatures with fast kinetics. Desorption times of a few minutes have been demonstrated[74,75]. High-entropy alloys have similar storage properties, but have a wide range of compositional variation, allowing the thermodynamics of hydrogen absorption and desorption to be finely tuned[69]. Using light elements in high-entropy alloys could also increase gravimetric capacities, compared with intermetallics containing relatively heavy components, combined with high potential hydrogen-to-metal ratios[71]. By contrast, complex hydrides tend to have a higher hydrogen content, for example, 18.5 wt% for $LiBH_4$ (ref. 8), but often require higher temperatures owing to their greater stability, with ΔH typically above 35 kJ mol^{-1}, and they can suffer from poor reversibility. Approaches adopted to modify properties include the addition of catalysts, anion or cation substitutions, nanoconfinement or mixed hydride systems, known as reactive hydride composites.

When doped with Ti-based catalysts, for example, $NaAlH_4$ is reversible with two decomposition steps below 200 °C (Fig. 3a). Its theoretical reversible capacity is 5.6 wt%, with nearly 5 wt% demonstrated experimentally[6,76,77]. Reactive hydride composites such as $MgH_2 + LiBH_4$ or $LiH + Mg(NH_2)_2$ can lower enthalpies and achieve reversibility in complex hydrides as a result of the formation of thermodynamically favourable phases[78,79]. Nanoconfinement within inert host materials can also alter both the thermodynamics and the kinetics[80–82]. Magnesium-based hydrides, in particular, have attracted considerable interest[83,84]. MgH_2 has mixed ionic–covalent Mg–H bonds, characterized by a high ΔH of 74.5 kJ mol^{-1} and a gravimetric capacity of 7.6 wt%[5,74], while the complex hydride $Mg(BH_4)_2$ has a hydrogen content of 14.8 wt%, with a reversible capacity of 11.4 wt%, though at high temperatures and pressures[85].

Hydrogen is absorbed and desorbed by metal hydrides via hydriding and dehydriding reactions. Such reactions are characterized by a variety of multiphysics processes, including chemical-bond breaking, diffusion and phase evolution. These processes are difficult to deconvolute experimentally yet define the overall reaction rates, as well as other important performance factors such as cyclability and initial activation. Chemo-mechanical effects at the interface boundaries become important because the reactions typically involve notable volume changes. Theoretical investigations based on density functional theory, multiscale modelling approaches and machine learning have provided insights into these governing mechanisms and their controlling factors, with a view towards rational materials design strategies based on sound physical understanding[86,87].

For stationary hydrogen storage, the capital expenditure required to store a kilogram of hydrogen is a key factor. Storage in hydrides is in competition with large-scale geological storage in salt caverns and conventional high-pressure storage vessels, with capital expenditure costs ranging from less than €10 per kg of H_2 for geological storage to €500–1,000 per kg of H_2 above ground[88]. Hydride storage can be cost competitive with aboveground compressed hydrogen storage and it has two key advantages — lower storage pressures and reduced system dimensions (as shown in a techno-economic analysis of hydrogen storage for microgrid applications)[89]. Commercial AB_2 and AB_5 alloys typically cost €20–80 kg^{-1}, depending on whether they contain expensive elements. Assuming an AB_2 alloy costing €20 kg^{-1} has a working capacity of 2 wt%, then the material cost would be €1,000 per kg of H_2, excluding the cost of the tank. Most commercial metal hydride tanks therefore contain cheaper AB alloys, such as those based on TiFe, for which the price strongly depends on purity and additional elements but are typically €7 kg^{-1} (ref. 90) or as low as €3 kg^{-1} using recycled Fe and Ti (ref. 91). By contrast, MgH_2 offers the combined advantage of high gravimetric capacity (working capacity approximately 6 wt%) and the low cost of Mg metal, around €3 kg^{-1} (ref. 90). Unfortunately, Mg-based hydrides typically require temperatures in excess of 350 °C for useful operational pressures and charging and discharging rates. An important advantage of solid-state storage with metal hydrides, compared with

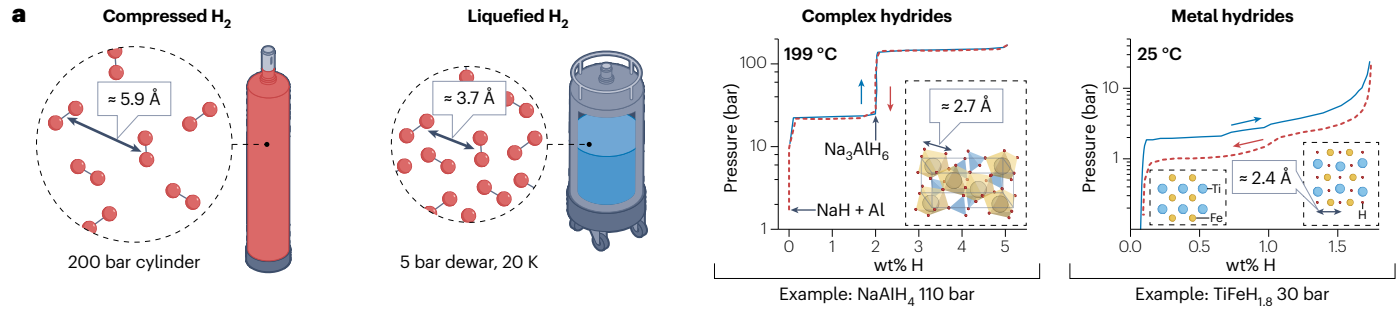

Fig. 3 | Hydrogen storage in complex and metal hydrides. a, The differences between volumetric hydrogen storage capacities for compressed gas at 16 g l^{-1}, a liquid hydrogen dewar at 70 g l^{-1}, a complex hydride store at 70 g l^{-1} and a metal hydride store at 105 g l^{-1}. $NaAlH_4$ has a higher gravimetric capacity than the metal hydride, but the locations for hydrogen in TiFe are closer together, resulting in higher volumetric density. The reaction pathway in the complex hydride example results in two distinct plateaus. Complex hydrides also often require higher temperatures and pressure to reversibly absorb hydrogen. The TiFe system has two plateaus representing the monohydride and dihydride phases, but many common metal hydrides exhibit a single phase change, resulting in a single flat or sloped plateau. Isotherm data for $NaAlH_4$ are replotted from ref. 237 and the TiFe isotherm behaviour illustrated using experimental data for $TiFe_{0.85}Mn_{0.05}$ are replotted from ref. 238. **b**, Metal hydride stores can be charged directly from commercial electrolysers with an output pressure of 35 bar without the energy cost associated with compression or liquefaction. However, thermal management is required owing to the large enthalpy change associated with hydrogen storage and release. From left to right: a thermal image of a metal hydride tank during charging with hydrogen using internal heat-transfer fins but no active cooling, illustrating the heat management of the system that is required. The schematics on the right show an example of system integration considerations when storing hydrogen from an electrolyser and delivering to a fuel cell, using a TiFe store as an example.

high-pressure gaseous hydrogen storage, which requires a mechanical compressor, is that they can be operated at low pressures such as that delivered direct from an electrolyser.

Thermal management is required for hydride stores to allow heat exchange during exothermic and endothermic hydrogen uptake and release (Fig. 3b). If a powder bed is used, short distances (1–2 cm) to the heat-transfer medium are required owing to the low effective thermal conductivity of powders, about 0.1 W m^{-1} K^{-1}. Pelletizing hydrides with graphite can increase the effective thermal conductivity to 10 W m^{-1} K^{-1} (ref. 92), although with a weight penalty. These additions must be considered when optimizing system designs using specific storage materials[93]. For stationary storage, system efficiency can be improved by integrating heat sinks or sources at the installation site. For example, the hydride tank can be combined with a thermal energy storage system based on phase-change materials, an approach used in the European-Union-funded HyCARE project to store about 50 kg of H_2 in 4 tonnes of a Ti–Fe–Mn alloy[11,94,95].

Stationary metal hydride stores can be used in fuel-cell-based emergency power systems[96], offering advantages such as low physical footprint and enhanced safety, compared with high-pressure tanks. Hydrogen desorption from metal hydrides is endothermic, so in the case of leakage, the hydride bed cools as hydrogen leaves the tank. Owing to a limited driving force and kinetics, a decreasing rate of hydrogen evolution is observed, reducing the required safety distances compared with high-pressure tanks[97]. Hybrid storage combining pressurized hydrogen with metal hydrides is another interesting application[98]. Calculations based on a case study of offshore hydrogen generation showed that hybrid storage can offer a volumetric density up to five times greater when using less than 10% by volume of a metal hydride, compared with compressed gas alone[99].

Mobile metal hydride storage systems are ideal for applications in which system weight (from the mass of the host metal) is not critical or is even an advantage (acting as ballast). Such applications include forklifts[100,101], submarines[102], rail[103] and waterborne transport[104]. In the latter, hydride tanks offer a simplified refuelling infrastructure and a substantial cost reduction compared with compressed or liquefied hydrogen. Hydrogen can also be transported safely at ambient pressure and temperature using metal hydrides. Tanks containing 15.6 tonnes of Mg-based alloy pellets, for example, can store 1.1 tonnes of H_2, fitted in a standard-size shipping container[105]. Reactive hydride composites, including complex hydrides, have the potential to deliver high-weight-per-cent hydrogen content at low pressures, which would satisfy most terrestrial and seaborne transport applications. There is therefore a continued push towards the discovery of reactive hydride composites that are reversible at near-ambient temperature.

To scale up hydride-based hydrogen storage, sustainable and recyclable systems must be demonstrated, while also considering cost. It is also important to work with stakeholders to ensure the social acceptability[106] of the technology[107].

Liquid hydrogen carriers

Hydrogen can also be stored and transported at ambient temperatures bound in hydrogen-rich liquids. Catalysts are required to release hydrogen from liquid carriers and purification is generally necessary[108]. A distinction can be drawn between LOHCs and other liquid carriers, such as ammonia, because LOHCs remain as liquids in both their hydrogenated and dehydrogenated forms, usually without binding or releasing gases such as N_2 and carbon dioxide (CO_2) from or to the atmosphere[108]. A key consideration for liquid hydrogen carriers is the thermodynamics of dehydrogenation, which is generally defined by the enthalpy of H_2 release, ΔH (ref. 45) (Fig. 4a).

Liquid organic hydrogen carriers

LOHCs include hydrocarbons, such as methylcyclohexane[109] and H18-dibenzyltoluene[110], as well as alcohols[111] and aqueous formate solutions[112]. LOHCs can be stored in unpressurized tanks at ambient temperature for long periods, because hydrogenation and dehydrogenation take place only within catalytic reactors (Fig. 4b). Choosing suitably sized tanks and reactors allows flexible decoupling of energy and power. Gravimetric storage capacities are typically in the range 4–7 wt%, presenting a challenge for onboard hydrogen storage, especially for light-duty vehicles[113,114]. Volumetric capacities, on a material basis, vary more widely. Formic acid and aromatic hydrocarbons have volumetric hydrogen densities of >50 g l^{-1}, around 70% that of liquid hydrogen (refs. 113,114). These properties, together with safety considerations, mean that LOHCs are well suited to large-scale, long-duration energy storage[113,114].

Homocyclic aromatic hydrocarbons are the most technologically mature LOHCs[109], but they have a relatively large ΔH, around 65 kJ mol^{-1}, which reduces the overall energy storage efficiency. Introducing heteroatoms to the hydrocarbon rings[115] can reduce ΔH. An example is H12-N-ethylcarbazole[116], with a ΔH of 53 kJ mol^{-1}. The fully dehydrogenated product is solid, however, at ambient temperature, so complete dehydrogenation is avoided. Low-enthalpy LOHCs, which could have higher energy efficiency than hydrocarbons, are being investigated. An example is the Na phenoxide/cyclohexanolate pair[12], with a ΔH of 50 kJ mol^{-1}, which undergoes dehydrogenation at only 100 °C and can be fully hydrogenated using a Ru/Al_2O_3 catalyst at 150 °C under 30 bar of H_2, with a ΔH of 52 kJ mol^{-1}. Low-enthalpy LOHCs could also benefit from the development of low-temperature catalysts because the energy demand is not dominated by the enthalpy of reaction.

Alcohols also offer low ΔH routes for hydrogen storage. Dehydrogenating ethanol to ethyl acetate, with a ΔH of 36 kJ mol^{-1}, has half the enthalpy of hydrocarbons and a capacity of 4.4 wt% and 35 g l^{-1}. Process modelling has shown that an overall energy efficiency of 88% for the release and uptake of hydrogen can be achieved for the complete storage cycle[117], compared with 54–61% for aromatic hydrocarbons[118]. However, if the LOHC has to be moved from a centralized regeneration facility to a remote location, the total round-trip efficiency will be lower. Therefore, such high efficiencies might not be attained in all specific use cases. For example, the use of ethanol with a molecular hydrogenation/dehydrogenation catalyst has been investigated for seasonal storage of 5,000 kg of H_2 in a microgrid[111]. The volume of ethanol required (96 m^3) was less than half that required to store the same amount of hydrogen in 250 bar compressed tanks (420 m^3). However, the main obstacle to using ethanol and a molecular catalyst is the combined heating and cooling requirements associated with the reflux of vapours being produced. The heating requirements are more than 200 kW, in addition to around 190 kW of cooling, to produce the hydrogen required for 65 kW of electricity to be generated by a hydrogen fuel cell.

One approach to reducing the cooling demand (to keep the LOHC in the liquid phase) is to use an alcohol with a higher boiling point, such as 1,4-butanediol (BDO). Process modelling of the γ-butyrolactone–BDO cycle has been performed to compare liquid- and gas-phase dehydrogenation of BDO[119]. Although ΔH for dehydrogenation in the gas phase, at 35 kJ mol^{-1}, is lower than in the liquid phase, at 43 kJ mol^{-1}, this

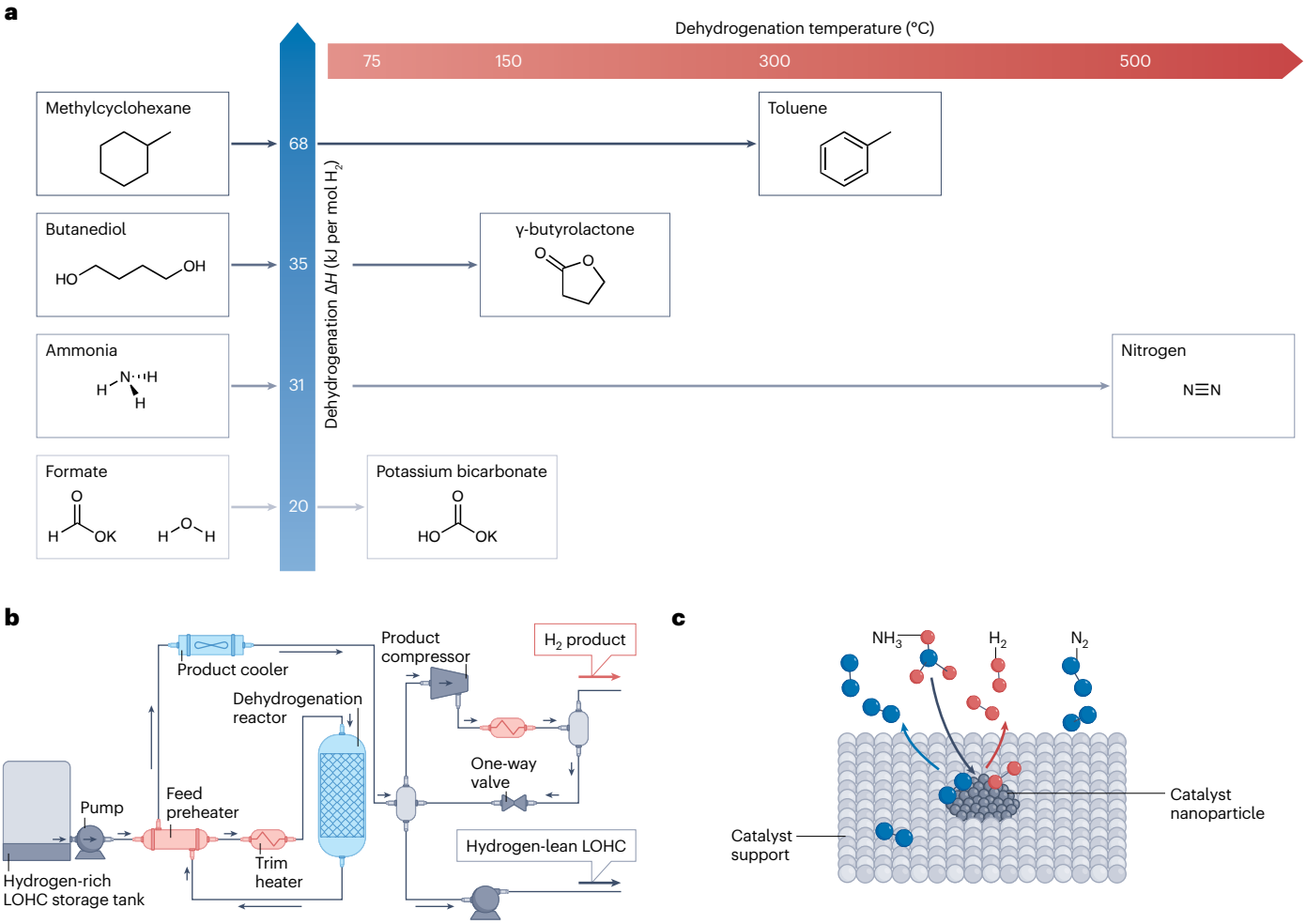

Fig. 4 | Hydrogen storage in liquid hydrogen carriers. a, The range of temperatures required to release hydrogen from ammonia and liquid organic hydrogen carriers (LOHCs). Dehydrogenation is favoured by low hydrogen pressures, so all examples are dehydrogenated at around ambient pressure. **b**, A schematic of an LOHC plant for dehydrogenation, which includes a material preheater to promote dehydrogenation, a reactor and a separator to collect the lean LOHC and hydrogen, together with subsequent compression. **c**, The catalysed chemical step for the release of hydrogen from ammonia. Ammonia is dehydrogenated by metal (such as Ru) nanoparticles on a carbon or metal oxide (TiO_2, SiO_2, Al_2O_3) support at about 500 °C. We note that LOHCs are dehydrogenated in an analogous manner using different metals/supports. ΔH, change in enthalpy. Panel **c** adapted from ref. 239, Springer Nature Limited.

is offset by the enthalpy of vaporization. Overall energy efficiencies of 75–78% were reported, regardless of whether liquid- or gas-phase dehydrogenation was used. Reaction conditions can therefore be chosen to favour other characteristics such as catalyst performance or reactor design.

Hydrogen storage using aqueous formate salts, with a ΔH of 20 kJ mol^{-1}, is attractive, particularly from the perspective of environmental safety. Hydrogenation to formate and dehydrogenation to bicarbonate can be performed using either thermocatalytic or electrocatalytic methods, adding to its versatility[120]. High-purity reagents are not required, with food-grade baking soda and tap water providing similar hydrogenation and dehydrogenation profiles to laboratory chemicals[121]. A key factor for successfully commercializing LOHCs is the stability and selectivity of catalysts[112]. Although product selectivities of >95% appear high, the remaining 5% of products present a challenge if they are not reversible and can lead to an increased levelized cost of storage. The levelized cost of storage using the γ-butyrolactone–BDO cycle has been investigated[122] and it was found that a loss of 5% of γ-butyrolactone (that is, a catalyst selectivity of 95%) doubled the levelized cost of storage before additional costs for separation. Multiple cycles compound this: for example, 50% of the LOHC is lost to by-product formation after just 14 cycles of 95% selectivity.

LOHCs can also be used to purify hydrogen from crude and waste sources (including syngas and industrial tail gases) that contain impurities such as CO, CO_2, light hydrocarbons, N_2 and water[123,124]. Only hydrogen binds to the LOHC, but the catalysts used must be tolerant of the impurities[123]. A Cu-based catalyst, for example, can extract hydrogen from mixtures of H_2, CO, CO_2, CH_4 and N_2. H_2 reacts with an ester to make an alcohol, that is, γ-butyrolactone to BDO, and the CO and CO_2 pass through the reactor, separating the H_2 without the need for a membrane or other separation methods[124].

Ammonia

Ammonia is currently being considered as a hydrogen carrier for long-distance transportation and as a CO_2-free fuel for combustion engines. Ammonia production via the Haber–Bosch process, however, is responsible for about 1.4% of global CO_2 emissions and around 1–2% of global energy consumption[125–127]. Depending on the hydrogen source and production method, CO_2 emissions per kg of NH_3 can vary considerably[128]. For example, the specific emission intensity of conventional large-scale ammonia plants in China is >5 tonnes of CO_2-equivalent (per tonne of NH_3) when coal is used as the hydrogen source but <3 tonnes of CO_2-equivalent when natural gas is used[129]. These figures align closely with those published by the International Energy Agency in 2021 (ref. 130). Global emissions from ammonia production based on coal are estimated to be 3.2–4.5 tonnes of CO_2-equivalent, and even the most efficient steam reforming processes emit about 1.6–1.8 tonnes of CO_2-equivalent. However, carbon capture could be one way to reduce emissions to 0.1–0.2 tonnes of CO_2 (ref. 131).

For ammonia to be a viable future energy carrier, it is essential to use green hydrogen for production and to develop alternative, low-energy synthesis routes. Endothermic ammonia decomposition requires high temperatures for sufficiently high reaction rates and high-purity hydrogen. As with synthesis, innovative strategies and novel efficient catalysts must be developed for decomposition. New approaches for both ammonia synthesis and decomposition are therefore required.

N_2 is an inert molecule with a N≡N bond energy of 942 kJ mol^{-1}. Ammonia synthesis from N_2 and H_2O or from N_2 and H_2 is thermodynamically and/or kinetically difficult. Exploring green ammonia production driven by light, electricity and plasma is at the forefront of catalysis research[132]. Promising progress has been made, for example, in the electrochemical nitrogen reduction reaction mediated by Li/Li_3N (refs. 13,133).

Reducing N_2 to NH_3 requires a supply of electrons and protons. Because the H^- in alkali and alkaline-earth metal hydrides is an electron and proton carrier, these metal hydrides are promising catalysts for green ammonia synthesis[134]. Furthermore, alkali or alkaline-earth metal cations can stabilize $-N_xH_y$ intermediates, thus lowering kinetic barriers during transformation. In thermocatalytic NH_3 synthesis, an unconventional nitride-hydride catalyst (BaCrNH) and complex hydride catalysts (Li_4RuH_6 and Ba_2RuH_6) have been developed that perform well under relatively mild conditions of 300 °C and 10 bar[135,136]. These electron-rich, multi-component catalysts favour non-dissociative N_2 activation and lattice hydride-involved hydrogenation, which is a different reaction mechanism from conventional Fe or Ru-based catalysts. In addition, LiH (a semiconductor with a bandgap of 3.7 eV) undergoes photolysis under ultraviolet irradiation, producing hydrogen and an electron-rich surface. This behaviour makes LiH catalytically active for photo-driven ammonia synthesis under ambient conditions[14].

In most cases of ammonia synthesis, metal hydrides are used in combination with transition metals. However, some metal hydrides have good catalytic activity under moderate conditions without transition metals. For example, potassium hydride intercalated in graphite (potassium hydride carbide; KH_xC_y)[137] is active in ammonia synthesis at 300 °C and 10 bar without a transition metal. Transition-metal-free catalysts activate N_2 via an associative mechanism rather than the dissociative mechanism, hence lowering the overall energy barrier for ammonia synthesis, because the N_2 is not dissociatively adsorbed on the catalytic surface.

One option to avoid conventional thermal ammonia decomposition (Fig. 4c) is to use ammonia for direct solid oxide fuel cells. This approach combines ammonia cracking over a Ni catalyst and the electrochemical conversion of hydrogen into electricity[138]. Ammonia can be fed directly into the solid oxide fuel cell, but microstructural deformation of the metallic anode owing to nitridation by the reaction with ammonia has been reported, which requires engineering solutions[139]. Combined ammonia decomposition and hydrogen separation is also possible using catalytic membrane reactors. These reactors operate at lower temperatures compared with conventional crackers but also at higher pressures, favouring selective separation of hydrogen from the reaction zone[140]. However, the purities of <0.1 parts per million NH_3 required for proton exchange membrane fuel cells cannot be realized without using Pd-based membranes or adsorbents such as zeolite 13X or clinoptilolite[141].

Plasma-assisted hydrogen generation from liquid ammonia is another technology for large-scale applications, providing a complete conversion of ammonia. Different methods of plasma generation, such as pulsed plasma or dielectric barrier discharges, have been combined with transition-metal catalysts[142]. Electrochemical decomposition (electrolysis) of liquid ammonia theoretically requires less energy than water electrolysis[143,144]. During decomposition, ammonia is oxidized at the anode to N_2, while H_2O is reduced at the cathode to H_2. The anodic reaction, however, competes with the side reaction of oxygen evolution. Electrochemical ammonia oxidation is promising for on-demand hydrogen production, but efficient, durable catalysts are key to the process: developments in this area include face sensitivity, alloying, metal–support interactions, and non-precious metal activation[145]. Mechanistic in situ and/or operando characterization studies of ammonia decomposition reactions are required to understand the complexity of the reaction mechanism, depending on the different approaches and variety of catalysts[146–149].

Hydrogen compression

In addition to the storage and transportation of hydrogen, other aspects of hydrogen handling are important. A key issue is that hydrogen technology for storage and transportation often requires high-pressure hydrogen gas. Fuel cell cars, for example, currently use 700 bar type IV tanks, so a hydrogen supply over 700 bar is required at refuelling stations. Metal hydrides offer an efficient alternative to conventional compressors for achieving such pressures[150,151].

Hydrogen can be compressed using various methods, including mechanical, electrochemical, thermal and thermodynamic compression. Mechanical compressors reduce the volume containing the gas or force gas into a smaller volume, thus increasing pressure[152]. These compressors include syringe pumps and reciprocating compressors, which move a solid piston into the gas space; rotary compressors, which use a rotating screw to force gas into a pressure chamber; and ionic compressors[153], which pump an ionic liquid into the gas space. Electrochemical compressors use a proton exchange membrane that dissociates H_2 at the anode and recombines it at the cathode at a higher pressure[154], whereas in thermal compression, low-temperature gas is heated in a fixed volume. Metal hydride compression, by contrast, uses the thermodynamic properties of a metal–hydrogen system to absorb hydrogen at a low temperature and release it at a higher pressure when heated (Fig. 5). Each method has advantages and disadvantages. Reciprocating compressors are widely used because they are simple and relatively inexpensive, but metal hydride compressors have the advantages of no moving parts, no vibrations and

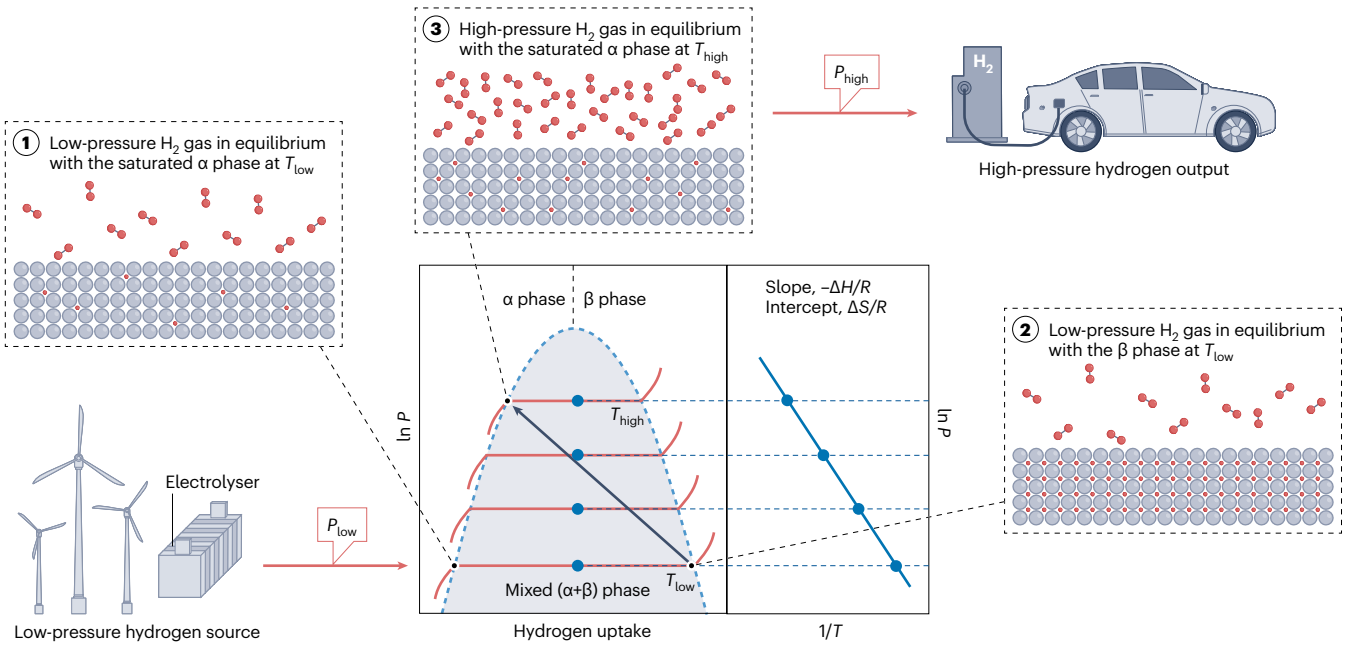

Fig. 5 | Hydrogen compression using metal hydrides. Schematic of a single-stage metal hydride compressor. Low-pressure hydrogen from an electrolyser, for example, driven by wind turbines or another renewable energy source is fed into the metal hydride compressor at a low temperature T_{low} and hydrogen is absorbed into the metal crystal structure, forming the alpha (α) solid-solution phase. The hydrogen uptake increases, as seen in the plateau of the lowest temperature isotherm, until the maximum capacity is reached and the absorbed hydrogen is all in the beta (β) hydride phase. Then the metal hydride is heated using waste or low-grade heat where possible. The hydrogen is released from the metal at a higher temperature T_{high} and a higher pressure P_{high}, suitable for a hydrogen refilling station or other applications. ΔH, enthalpy of the α-to-β phase transition; ΔS, entropy of the α-to-β phase transition; P, pressure; R, universal gas constant; T, temperature.

low maintenance. Another advantage is the purity of the compressed hydrogen, thanks to the absence of oil and other lubricants and to the trapping of impurities, such as H_2O and O_2, by the metal hydride. Maintaining high hydrogen purity is important because fuel cells are sensitive to impurities and minimum purity standards must be met to prevent fuel cell poisoning.

When a hydride is formed from a metal and hydrogen gas, heat is released. Conversely, when a hydride is heated, hydrogen gas is released. By increasing temperature, pressure can therefore be amplified (Fig. 5). This amplification can reach several hundred bar, even if the operating temperature is limited to 150 °C, which can be provided by steam from waste heat at chemical plants. This heating requirement is a disadvantage of metal hydride compressors, as is the need to remove heat generated during the absorption cycle, but using waste heat and effective thermal management can improve efficiency and kinetics. For comparison, heating hydrogen gas from 20 °C to 150 °C increases the pressure by only 44%, while an exponential temperature-dependent pressure increase for metal hydride systems is approximately 20 times more efficient, allowing pressures exceeding 800 bar to be achieved. Modelling metal hydride compressors to assess the performance of materials from the viewpoint of the thermodynamics of hydrogen–metal interactions shows their operation to be feasible over a broad range of pressures[15].

Hydrogen can be compressed in a single-stage metal hydride compressor, using two setpoint temperatures (T_{low} and T_{high}) to compress hydrogen from P_{low} to P_{high} (Fig. 5), or in a multistep process where two or more compression stages are synchronized[155,156], gradually increasing pressure from a setpoint level at ambient temperature. For efficient compression, a material should exhibit an isotherm with a flat plateau, with minimal hysteresis between absorption and desorption, and a low range of solid solutions in both α and β phases. The material must also have high cyclic stability, under elevated temperature and pressure conditions, and exhibit rapid absorption and desorption kinetics. Cyclic stability is a particular issue for metal hydride compression because material degradation processes[157], primarily disproportionation, where one or more metallic element phases segregate, are more prevalent under pressure at elevated temperatures. The compressor must also provide a minimum throughput of hydrogen for the particular application.

Since compression to different pressures is required, particularly in multi-stage compressors, various hydride-forming materials with different thermodynamic stabilities have been investigated[11,60,150]. AB_5 compounds, typically $LaNi_5$ and its derivatives, can be used in low-pressure compressors (up to 100 bar), whereas higher pressures (100 to 1,000 bar) can potentially be achieved using AB_2 compounds, often Ti-based Laves-phase intermetallics[150]. The sensitivity of the thermodynamics of a metal–hydrogen system to the composition of the alloy is such that materials can be tuned via partial substitution, so that they absorb and desorb hydrogen in the required pressure and temperature range[11,60,158].

To assess materials, experimental data are typically collected up to 100 bar and at temperatures below 150 °C, and achievable pressures are estimated using the van't Hoff equation (Box 1). However, research has been shifting to higher pressures (in the range 700–1,000 bar)

to satisfy requirements for hydrogen refuelling stations. Measurements must be made with great care at these pressures, because experimental issues and artefacts such as leaks[159], the internal volumes of valves, and sample volume changes during absorption and desorption[160,161] become even more critical for obtaining reliable data, as does using the fugacity or hydrogen equation of state to predict accurate pressures[158,162].

As part of the focus on higher pressures, compounds capable of hydrogen compression up to 800 bar, such as $Ti_{0.8}Zr_{0.2}Fe_{1.6}V_{0.4}$, have been identified[159] and prototype compressors producing more than 700 bar have been developed[17,18]. For example, a single-stage laboratory compressor capable of compressing hydrogen from 100 bar to 700 bar using a Ti-based AB_2 intermetallic has been reported[18]. In addition, a prototype double-stage metal hydride compressor for amplifying hydrogen pressure from 150 bar to 875 bar was demonstrated[17] using $TiCrMn_{0.7}Fe_{0.2}V_{0.1}$ for the low-pressure stage and $Ti_{0.8}Zr_{0.2}Fe_{1.6}V_{0.4}$ for the high-pressure stage. In both cases, the hydrides were mixed with expanded natural graphite to increase thermal conductivity.

For multi-stage compression, materials must be paired appropriately[156]. A model of a double-stage compressor has been developed in order to calculate the cycle productivities of the paired materials, intermediate pressures between the stages, and total throughput. Results agreed well with those from an experimental compressor[16]. Techno-economic analyses for metal hydride compressors also show that the capital expenditure is comparable to that for conventional mechanical compressors, but energy consumption can be lower, leading to higher energy efficiency and reduced operating costs, if waste heat is available[163,164]. In an integrated hybrid system comprising a metal hydride compressor and an electrochemical hydrogen pump, more waste heat was available from the pump than was required for the compressor, suggesting that operation using only waste heat should be possible[165]. The primary disadvantages of metal hydride compressors are potential material degradation, the slow kinetics (which will limit throughput) and the need for effective thermal management. Therefore, both materials development (such as compositional tuning and improving cyclic stability) and tank design (including thermal management and efficient waste-heat utilization) should be addressed in order to further develop metal hydride compressor technology.

Electrochemical energy storage

Metal hydrides have played a key role in electrochemical energy storage, as reversible negative electrodes in nickel-metal hydride (Ni-MH) batteries[166]. The proof of concept of Ni-MH batteries was first demonstrated in the early 1970s. They came to market two decades later[167] and were in widespread use in hybrid electric vehicles by the 2010s[2,168,169]. For most applications, Li-ion batteries have now overtaken Ni-MH technology. The liquid organic electrolytes in Li-ion batteries allow the use of electrode pairs that provide a larger potential difference than those used with aqueous electrolytes in Ni-MH batteries, but they also introduce safety issues, because the organic electrolyte is flammable. SSBs, by contrast, offer an alternative with the potential to improve safety, energy density and sustainability[170]. New phenomena that enhance cationic mobility in complex hydrides for use as solid electrolytes have been discovered, leading to the first inorganic rechargeable magnesium

Box 1 | Metal hydride fundamentals

Metal hydrides are formed by the direct reaction of hydrogen gas with a metal[61–63]. The resulting bonds can be covalent, ionic or metallic, depending on the nature of the element or alloy. These chemical bonds are relatively strong, so hydrides are often formed at near-ambient temperature or above. When a metal is exposed to hydrogen, at a given temperature, H_2 molecules first dissociate on the surface and then H atoms enter the metallic phase in solid solution, usually known as the α phase. With increasing pressure, the hydrogen concentration in the solid solution increases until an ordered, higher-concentration metal hydride phase, known as the β phase, begins to nucleate. Because a new phase is present, the system loses a degree of freedom and the pressure remains constant until all the solid-solution α phase has been transformed to the ordered β phase. This phase transformation is the origin of the plateau in pressure–composition isotherms and it has practical consequences because a small change in pressure results in the material absorbing or desorbing large quantities of hydrogen.

The plateau pressure at any given temperature T is given by the van 't Hoff equation[61–63],

$$\ln\frac{P_{H_2}}{P_0} = -\frac{\Delta H}{RT} + \frac{\Delta S}{R}$$

where P_{H2} is the equilibrium pressure of hydrogen, P_0 is the reference pressure, usually 1 bar, ΔH and ΔS are the enthalpy and entropy of the phase transition, respectively, and R is the universal gas constant. At high pressures, P should be replaced by fugacity, to account for non-ideal gas behaviour. Plotting $\ln(P_{H2}/P_0)$ against $1/T$ gives ΔH and ΔS for the reaction.

Most elements in the periodic table can bond with hydrogen. Except for a few elements, however, binary hydrides usually cannot satisfy the conditions required for practical applications, so intermetallic compounds are often used. In the field of metal hydrides, intermetallic compounds are usually formed by alloying a metal that easily forms stable hydrides (A) with another element that does not (B), leading to different stoichiometries, including A_2B, AB, AB_2 and AB_5 (ref. 62). Intermetallic compounds, as well as compositionally disordered hydrogen-absorbing alloys such as PdNi, are usually considered distinct from so-called complex hydrides[6]. Complex hydrides have the general formula $M_xN_yH_n$, where M is an alkali metal cation or cation complex and N is a metal or metalloid. The bonding is mostly covalent, rather than metallic.

For metal hydrides, when hydrogen enters the metal lattice, the unit cell volume increases, in some cases by up to 30%[83]. Because this expansion is reversible during hydriding and dehydriding, intermetallic compounds often decrepitate upon cycling, forming a fine powder. Another aspect with important implications for practical applications is the exothermic and endothermic nature of the hydrogenation and dehydrogenation reactions. Enthalpies of formation of metal hydrides are relatively high, so heat management is crucial to achieve absorption and desorption kinetics that satisfy practical requirements.

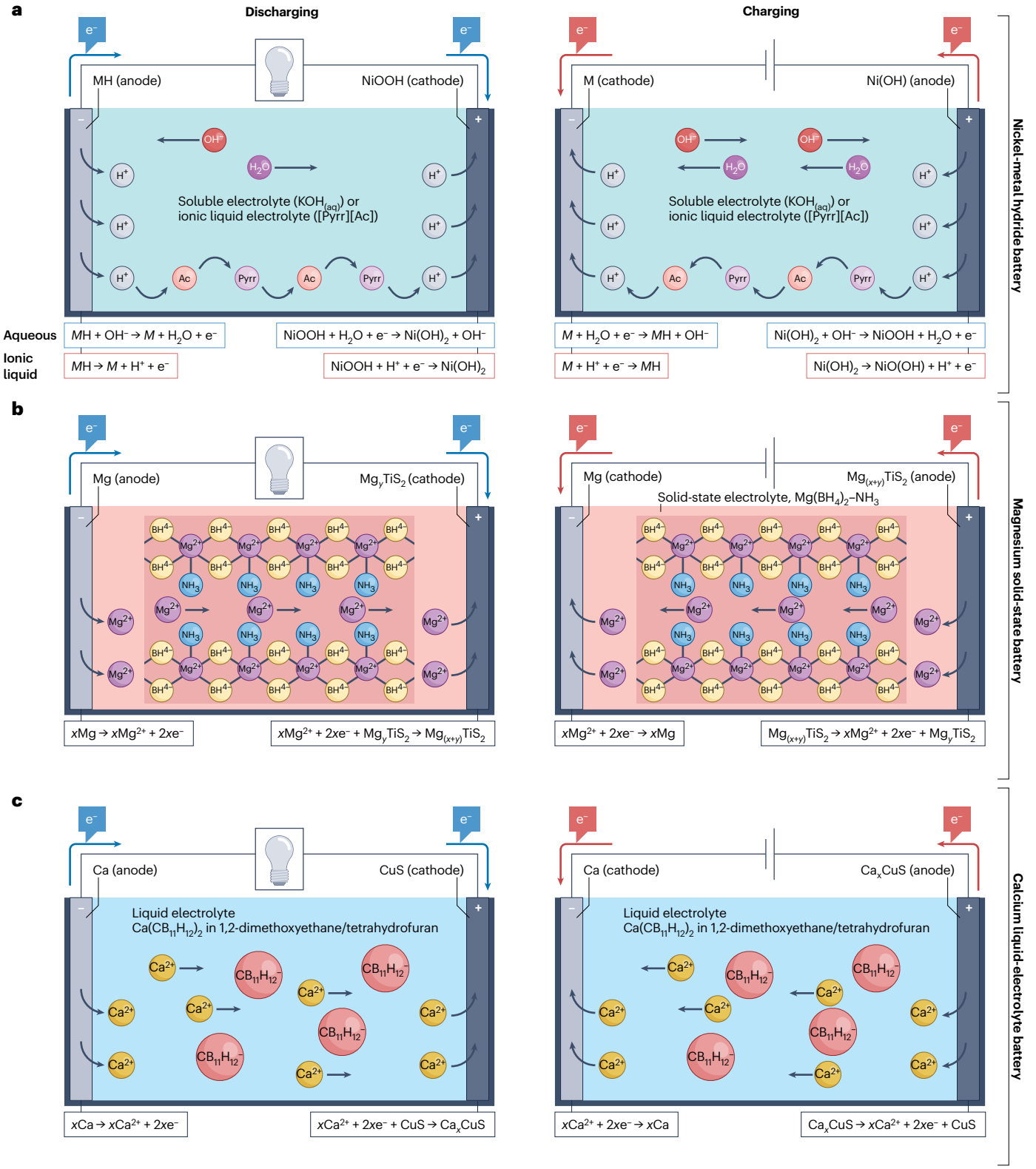

SSB[19]. Hydrides therefore could be promising for future generations of SSB[2]. In addition, complex hydrides show potential for use as liquid electrolytes in high-performance Mg- and Ca-based batteries. This section considers the improvement of existing Ni-MH technology, developments in hydride-based SSBs, and the use of complex hydrides as liquid electrolytes.

Fig. 6 | Hydrides for electrochemical energy storage. Rechargeable hydride-based batteries during discharge and charge steps. **a**, A nickel-metal hydride (Ni-MH) battery operating with a hydride-forming metal as the negative electrode, an aqueous alkaline or ionic liquid as electrolyte, and nickel hydroxide as the positive electrode. **b**, A magnesium solid-state battery with an Mg-metal negative electrode, magnesium tetrahydridoborate ammine ($Mg(BH_4)_2.NH_3$) as the electrolyte and a titanium disulphide positive electrode where the redox couple Ti^{4+}/Ti^{3+} allows insertion of Mg^{2+}. **c**, A calcium liquid electrolyte battery with a Ca-metal negative electrode, calcium monocarborane ($Ca(CB_{11}H_{12})_2$ dissolved in organic solvents as the electrolyte and a copper sulphide cathode as the positive electrode where the redox couple $Cu^{2+}/Cu0$ allows insertion of Ca^{2+}. The corresponding reactions are shown below each electrode.

Nickel-metal hydride batteries

Ni-MH batteries discharge via two processes (Fig. 6a). At the negative electrode, a metal hydride is oxidized to a metal (M), while at the positive electrode, nickel oxy-hydroxide, NiO(OH), is reduced to form nickel hydroxide, $Ni(OH)_2$. Proton (H^+) transfer between the electrodes occurs through a highly concentrated aqueous alkali electrolyte with high ionic OH^- conductivity (0.5 S cm^{-1} at room temperature for 8 M KOH). This aqueous electrolyte provides intrinsic safety and robustness, but it is corrosive and the narrow electrochemical stability window (1.23 V) constrains the energy density of Ni-MH batteries. For comparison, liquid organic electrolytes in Li-ion batteries can have electrochemical stability windows exceeding 3 V (ref. 171).

First-generation commercial Ni-MH batteries used multi-substituted $LaNi_5$-type intermetallics as negative electrodes; Co, Mn and Al partially substitutes Ni, while La is replaced by mischmetal, a mixture of rare-earth elements with a composition depending on the ore[67,166]. Cycle life was improved, compared with pure $LaNi_5$, but cost was also reduced considerably. The success of metal hydride electrodes relies on their low potential (−0.95 V versus the normal hydrogen electrode), good gravimetric energy capacity (300 mAh g^{-1}), high electronic conductivity, fast hydrogen mobility at room temperature (hydrogen diffusion coefficient approximately 10^{-8} cm^2 s^{-1}) and the formation of a stable and ionic conducting surface electrolyte interphase formed by rare-earth hydroxides and catalytic nanostructured metals[172]. Second-generation commercial Ni-MH batteries[173] use $LaNi_5$–$MgNi_2$ intergrowth alloys, which were developed later, with capacities approaching 400 mAh g^{-1}. Energy density is increased, while reducing the use of strategic rare-earth elements[174].

Ultimately, using rare-earth-element-free alloys would be the ideal, particularly those based on lightweight Ti, V or Mg hydride-forming metals. However, cycle life has so far been poor owing to severe corrosion in alkali media[172]. Replacing aqueous alkali electrolytes with less aggressive alternatives while preserving fast hydrogen mobility is one solution for the next generation of Ni-MH battery technology. Protonic ionic liquids have been proposed and their ability to operate in batteries demonstrated using pyrrolidinium acetate [Pyrr][Ac] as the ionic liquid[175,176]. The electrochemical stability windows of ionic liquids are much larger than that of water, >2 V, paving the way towards the implementation of higher-potential positive electrodes approaching the high energy density of Li-ion batteries.

Complex-hydride-based SSBs

SSBs are on the current roadmaps of various battery companies and car manufacturers because they have several advantages over liquid-state Li-ion batteries[177–179]. Battery cells consisting only of solids should be easier to assemble, reducing fabrication cost, and they should be smaller, lighter and have higher energy density. A solid electrolyte can eliminate the flammable and unstable liquid electrolyte used in Li-ion batteries, improving safety and lifetime. Moreover, these electrolytes can operate over a larger temperature range and reduce the need for thermal management, allowing the battery to be operated with fast charging and discharging rates and reducing the risk of short circuits[170].

SSBs consist of two electrodes (a cathode and anode) and a solid cation-conducting electrolyte[170]. The ion-conducting electrolyte is the central part of the battery and its stability towards anode and cathode defines the battery chemistry. A challenge when developing SSBs is to achieve fast cationic conductivity in solid electrolytes, in particular for divalent cations such as magnesium (Mg^{2+}) or calcium (Ca^{2+})[180–182]. Traditional cation-conducting oxides and halides often have close-packed structures and have cationic conductivity only at high temperatures owing to defect formation. Derivatives of complex hydrides with a metal ion bound to a neutral molecule provide fast cationic conductivity[19,183–185]. Classes of complex-hydride-based materials have been discovered that also have more open and flexible structures and 'zero' electronic conductivity[19]. These hydrides suggest routes to creating fast cationic conducting materials for SSBs.

An ammonia derivative of magnesium borohydride, $Mg(BH_4)_2{\cdot}NH_3$, has been discovered[19], which illustrates another phenomenon that increases the magnesium ionic conductivity, creating a functional battery material. The structure of $Mg(BH_4)_2{\cdot}NH_3$ is held together by weak di-hydrogen bonds, $B{-}H^{\delta-}\cdots{}^{+\delta}H{-}N$. This interaction resembles the hydrogen bonds in biological matter with a similar interaction energy, around 20 kJ mol^{-1}, and bond length, around 2 Å. Density functional theory calculations revealed that the fast cationic conductivity is due to these weak interactions, flexible coordination of the BH_4^- complex, and exchange of the neutral molecule (NH_3) between interstitial and framework magnesium. This mechanism is referred to as ligand-assisted cationic conductivity, and it could be unique to hydride-based electrolytes[19]. Boron-based complex hydrides have low material density and are relatively soft and compressible, forming stable interfaces to the electrodes[2,180,186]. Furthermore, they are slightly reducing and stable towards metallic anodes, which can further increase energy density[187].

The first rechargeable inorganic magnesium SSB was assembled using magnesium borohydride complexed with tetrahydrofuran as the electrolyte, magnesium metal foil as the anode, and titanium sulphide as the cathode (Fig. 6b). The drawback is the relatively low oxidative stability of tetrahydridoborate (BH_4^-), which allows only low-potential cathodes providing a cell voltage of about 1.2 V (ref. 188). This metal borohydride-based electrolyte system has now been extended to similar calcium borohydride derivatives with high Ca^{2+} conductivity[189]. Further work is needed to develop electrolytes based on *closo*-(car)borates, for example, $B_{12}H_{12}^{2-}$ or $CB_{11}H_{12}^-$ (refs. 190–192). Borates often form anion lattices with dynamic disorder, that is, rotation and/or vibration of the anions, which further promotes fast cationic conductivity. Closo-borate anions also have higher electrochemical stability than tetrohydridoborates and facilitate formation of high-voltage SSBs[193]. Future work could provide analogous calcium electrolytes and open the door to developing similar calcium-based SSBs.

Complex hydrides as liquid electrolytes

Using complex hydrides as liquid electrolytes has also emerged as a strategy to overcome the challenges associated with traditional liquid electrolytes. An initial success was the development of a Mg battery electrolyte, $Mg(BH_4)_2$ and $Mg(CB_{11}H_{12})_2$ dissolved in ether solvent[194,195]. This electrolyte demonstrated excellent performance for Mg-metal plating/stripping reactions, exhibiting low overpotentials and high-quality deposition, making it a strong candidate for Mg batteries. This application highlights the potential of complex hydrides to address issues such as high overpotentials and poor cycle stability, which frequently occur in multivalent cation-based systems[196,197].

In Ca batteries, the complex hydride $Ca(CB_{11}H_{12})_2$ also shows promise as an electrolyte. When dissolved in a mixture of solvents, such as 1,2-dimethoxyethane and tetrahydrofuran, $Ca(CB_{11}H_{12})_2$ provides a wide electrochemical stability window of over 4 V and high ionic conductivity of 4 mS cm^{-1}, facilitating reversible Ca plating/stripping at ambient temperature. This electrolyte improves the stability of liquid electrolytes with Ca metal, enabling long-cycle-life Ca batteries[198]. Batteries using $Ca(CB_{11}H_{12})_2$ and a CuS cathode (Fig. 6c) have shown excellent cycle life and capacity retention, with up to 92% capacity maintained after 500 cycles, making them a potential alternative to Li-ion batteries[199].

Another approach is to use polymer electrolytes, such as gel polymer electrolytes, incorporating complex hydrides. Gel polymer electrolytes consist of a liquid electrolyte immobilized in a polymer matrix. These electrolytes have improved electrochemical properties and stability compared with traditional liquid electrolytes, while mitigating risks such as dendrite formation and short-circuiting[200]. For example, a gel polymer electrolyte composed of $Li_2B_{12}H_{12}$, propylene carbonate and poly(methyl methacrylate) (PMMA), had high ionic conductivity and electrochemical stability[200]. $Ca(BH_4)_2$-based polymer electrolytes also have high Coulombic efficiency and low overpotentials, advancing the development of Ca batteries with improved performance and safety[201].

Thermal energy storage

Thermal energy storage has a vital role to play in a decarbonized future[202,203]. Around half of global energy consumption is estimated to be lost as waste heat[204–206]. If even a fraction of this can be recovered and either used directly or stored for future use, it could substantially reduce worldwide CO_2 emissions. Moreover, thermal energy storage can be combined with concentrated solar power plants[207], to address intermittency and improve the reliability of energy supply[208,209]. Metal hydrides have very high heat storage capacities and can be used over a wide temperature range, as required by different thermal energy storage applications.

Thermal energy can be stored in materials using different processes[206,210,211]. Sensible heat storage is a physical process that uses linear increases and decreases in the temperature of a material, ΔT, to store and release heat. Another physical process, latent heat storage, involves phase transitions[209]. By contrast, a third option, thermochemical energy storage (TCES)[211], exploits reversible chemical reactions such as the absorption and desorption of hydrogen by metals[20,212] (Fig. 7a). Other TCES systems include metal hydroxides and carbonates[206,213]. TCES generally provides higher storage densities than sensible or latent heat[208,213], but some metal hydrides have the highest energy densities of all currently known thermochemical systems[211].

At present, concentrated solar power plants use molten salts to store sensible heat. Molten salts have gravimetric energy storage densities of around 0.045 kWh kg^{-1} for a ΔT of 100 K (ref. 210). 28,000 tonnes of molten salt is therefore required to store 1,000 MWh, but the same amount of heat can be stored using 1,100 tonnes of Mg (ref. 214). Metal hydrides can also cover a wide range of temperatures up to 1,000 °C, depending on the metal or metal alloy (Fig. 7b). The endothermic reaction associated with hydrogen desorption from the hydride is used to store heat, which can then be released by reacting hydrogen with the metal. Heat released during the exothermic reaction is collected using a heat-transfer medium and delivered to a heat engine, such as a turbine or Stirling engine, to produce electricity (Fig. 7a). The hydrogen is not combusted by reaction with oxygen, as in a fuel cell, but acts as a working medium to store or release chemical energy[213]. If reversible metal hydride TCES systems are connected to hydrogen sources, such as hydrogen pipelines, an option would be to use them not only for heat storage, but also for temporary hydrogen storage in a future hydrogen economy.

Selection of the metal hydride for the required working temperature is critical for TCES, as is achieving a high cyclic stability under the operating conditions[209]. The price of the material must also be low given that this will directly affect the system cost (capital expenditure)[215–217]. Hydrides being considered for TCES include MgH_2, Mg_2FeH_6, $NaMgH_3$ and CaH_2 and various derivatives, depending on the required working temperature[212,216]. In each case, the reaction enthalpy ΔH (in moles of H_2) determines the working temperature and the gravimetric energy storage density in terms of kilograms of reactant (that is, the weight of hydride, which depends on both the hydrogen content and molar mass of the host metal or metal alloy).

At lower working temperatures (up to 400 °C, which includes high-grade industrial waste heat), MgH_2 is an attractive choice because of the low price of Mg and its high heat storage capacity. The ΔH for MgH_2 (74.5 kJ mol^{-1}) corresponds to a gravimetric energy density of 0.78 kWh kg^{-1}. MgH_2 was first used to store heat more than 40 years ago[218]. Since then, numerous studies have been performed to optimize its kinetics, storage capacities, heat conductivity and long-term stability[84,214]. As MgH_2 has an equilibrium pressure of less than 10 bar from 350 °C to 380 °C, it can be used under relatively simple technical conditions. This usability has been shown in a demonstration project, commissioned in 2022, using 350 kg of Mg metal – with 5 wt% Fe powder added as catalyst – to store up to 250 kWh of heat, providing an energy density of 0.71 kWh kg^{-1}, close to the theoretical value. Heat input and removal was performed with an oil circuit[20] (Fig. 7c).

For working temperatures up to 550 °C, Mg_2FeH_6 has high cyclic stability and a ΔH of 77 kJ mol^{-1}, corresponding to an energy density of 0.55 kWh kg^{-1}. Decomposition of Mg_2FeH_6 releases three moles of H_2, with Mg and Fe metal formed as decomposition products. Mg and Fe do not form alloys with one another, so the two phases separate. This separation prevents sintering, which is often observed for other metal hydrides after long-term cycling[219]. $NaMgH_3$ has a higher ΔH of 86 kJ mol^{-1}, resulting in a dissociation pressure of about 1 bar at 500 °C (ref. 213), compared with about 66 bar for Mg_2FeH_6. However, the energy density for the first usable reaction step of 0.47 kWh kg^{-1} is lower than for Mg_2FeH_6. A drawback for $NaMgH_3$ is that full hydrogen desorption results in molten Na-metal segregation with poor kinetics during hydrogen reabsorption[215]. In an effort to find other suitable materials in the 500–800 °C range, fluorine has been used to stabilize NaH[220,221], MgH_2 (refs. 222,223) and $NaMgH_3$ (ref. 215). Although these materials can operate up to 775 °C at 150 bar, evaporation of Na must be eliminated for practical applications[212].

At high temperatures (up to 1,000 °C), CaH_2 is one of the best hydrides for TCES. Its ΔH is 216 kJ mol^{-1}, corresponding to a gravimetric energy density of about 1.43 kWh kg^{-1}. CaH_2 reaches an equilibrium pressure of 1 bar at about 1,000 °C, where it is in the molten state[224],

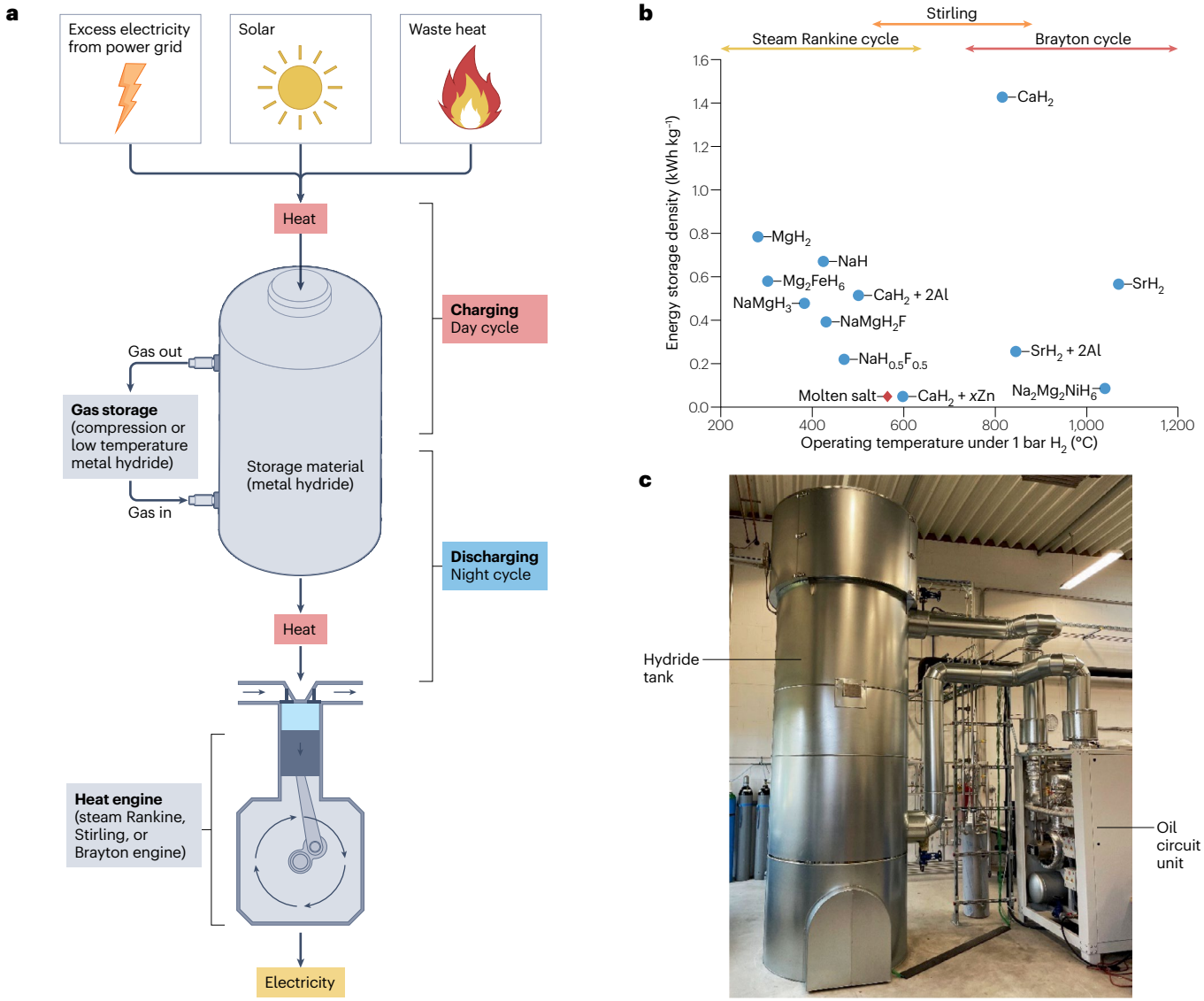

Fig. 7 | Thermal energy storage using metal hydrides. a, System for storing renewable energy, depicting the charging (day) cycle of the metal hydride and the subsequent release (and storage) of the hydrogen gas, and the discharge (night) cycle where the hydrogen gas is resupplied to the metal hydride to produce heat. This heat then drives an engine to produce electricity. **b**, Energy storage densities and operating temperatures of selected metal hydrides under 1 bar H_2 pressure, including the heat engine suitable for electricity generation at the operating temperature of the material. Molten salt is also shown for comparison. **c**, Heat storage demonstration unit filled with 350 kg of Mg to store 250 kWh at a temperature of approximately 350 °C. The oil circuit unit used to pump the heat-transfer fluid is also shown.

which makes heat transfer more favourable than for a powder. However, the corrosivity of molten CaH_2 and the slow kinetics must be overcome. Systems are therefore being sought to improve the kinetics of hydrogen absorption and release and to adjust the working temperature. Adding Al to CaH_2 reduces operating temperatures to <700 °C (refs. 225,226), and this CaH_2–Al system has good cyclability and low cost for operation at temperatures between 420 °C and 700 °C. For example, at 670 °C and 20 bar, the CaH_2–Al system has been cycled up to 66 times, although with a drop in capacity of 9%[226]. Other systems studied for TCES include CaH_2 destabilized by halides[227], Al_2O_3 (ref. 228), Zn (ref. 229) and Si (ref. 230).

Heat input and output are important criteria for practical implementation[206]. Depending on the hydride and its working temperature, various options are available. Heat-transfer oils are often used up to 400 °C (ref. 217). Heat extraction and delivery using superheated water vapour has been demonstrated for $NaMgH_3$ at temperatures up to 470 °C (ref. 231). Up to 600 °C, molten salts are suitable, whereas supercritical CO_2, molten alkali metals, and heat conduction through metallic rods are all being investigated for temperatures >600 °C.

For improved TCES systems, new metal hydrides should be investigated and their thermodynamic properties thoroughly characterized.

Glossary

Absolute adsorbed quantity
Total amount of hydrogen in the adsorbed phase, that is, the total quantity of hydrogen adsorbed by a porous material.

Alloy
A metallic material or solid composed of a mixture of two or more metals, or of metals and non-metal or metalloid elements.

Brunauer–Emmett–Teller method
The Brunauer–Emmett–Teller method determines the surface area of materials by analysing gas-adsorption isotherm data using a simplified model of adsorption.

Excess adsorbed quantity
Amount adsorbed over and above the amount of hydrogen that would be present in the absence of any gas–solid interactions.

Gravimetric density
In the context of hydrogen, the amount of hydrogen stored per unit mass.

Green hydrogen
Hydrogen produced from renewable energy sources, usually by the electrolysis of water, resulting in very low or zero carbon emissions.

Intermetallic compound
A long-range-order alloy, with a structure differing from those of its constituent elements, which are often present in stoichiometric quantities.

Mischmetal
A mixture of rare-earth elements, with a composition depending on the ore used for its production, often used to replace pure La in AB_5 intermetallic compounds.

Type III tanks
High-pressure gas cylinders, suitable for storing hydrogen, each consisting of a metal alloy liner wrapped in a carbon fibre composite.

Type IV tanks
High-pressure gas cylinders, suitable for storing hydrogen, each consisting of a polymer liner wrapped in a carbon fibre composite.

Usable capacity
Reversible hydrogen uptake between the pressure at which a hydrogen store is charged and the discharge pressure.

Volumetric density
In the context of hydrogen, the amount of hydrogen stored per unit volume.

Heat transfer is crucial for heat storage, as it determines how quickly and efficiently energy can be transferred (charged) into and removed (discharged) from the storage unit. Therefore, methods and devices should be investigated to optimize heat transfer in TCES systems. It is now time to move from working with metal hydrides at the laboratory scale to demonstration projects, with subsequent integration into a variety of thermal processes.

Summary and future perspectives

In this Review, we have examined hydrogen storage and transportation using nanoporous materials, metal and complex hydrides, and liquid hydrogen carriers. High-surface-area MOFs can store over 10 wt% of hydrogen using physisorption, under moderate conditions between cryogenic liquid hydrogen and high-pressure compressed-gas storage. The rapid and fully reversible adsorption process enables quick filling and high cyclability, and is best suited to short-term applications. Hydrogen storage in metal hydrides, meanwhile, requires only moderate pressures and near-ambient temperatures. Volumetric hydrogen densities nearly twice that of liquid hydrogen can be achieved, although gravimetric storage capacities are low, typically <2 wt%, meaning it is better for stationary applications. By contrast, liquid hydrogen carriers, such as LOHCs and ammonia, are best suited to long-distance transportation and long-duration energy storage. However, they face several challenges, including efficient LOHC hydrogenation and dehydrogenation and green ammonia production and decomposition routes.

We also discussed hydrogen compression using metal hydrides, the current status of metal and complex hydride-based batteries, and thermal energy storage using hydrides. Metal hydrides can be used to compress hydrogen quietly and efficiently, while ensuring a high-purity supply. Prototypes have demonstrated the feasibility of achieving pressures >700 bar. Intermetallic hydrides have proved a commercial success as electrode materials in Ni-MH batteries, but new lightweight electrode materials and less aggressive electrolytes, such as ionic liquids, are required to compete with recent improvements in battery technology. Complex hydrides, meanwhile, have shown promise as both solid and liquid electrolytes in new types of Ca and Mg battery. Finally, thermal energy storage is set to have a vital role in the future, thanks to the quantity of waste heat produced globally and the promise of concentrated solar power plants for generating renewable energy in countries with high solar irradiance. Metal hydrides exhibit very high heat storage densities over a wide temperature range, with CaH_2 allowing working temperatures up to 1,000 °C.

For physisorption-based hydrogen storage, a key challenge is to increase the volumetric capacity while maintaining high gravimetric values. This aim could be achieved by optimizing pore structure and reducing void volumes in powders using monoliths and other structured forms, with the goal of approaching volumetric densities comparable to high-pressure type IV tanks. Scale-up of materials production is needed, with a focus on green chemistry and avoiding harmful solvents (Box 2). Demonstration tanks are also currently being developed, as implementing practical hydrogen storage systems in tanks for heavy duty vehicles or stationary stores is important in implementation. Life cycle assessments of physisorption-based hydrogen storage in different scenarios are also needed before these systems can be scaled up for use in practical applications. At subcritical temperatures, a super-dense molecular hydrogen layer has been observed to form on special surfaces. Elucidating the exact structures required for this layer formation will help to increase the volumetric capacity of cryogenic hydrogen storage systems.

Metal hydride hydrogen storage is especially suited to stationary applications and heavy-duty transport and could break through in other market segments if investment costs become competitive with those for compressed and liquid hydrogen storage. Circular economy approaches to producing hydrogen-sorbing alloys using recycled metals with lower purity could reduce the cost of alloy production, the main driver of the high capital expenditure for hydride-based storage. Accelerated material discovery methods are expected to unveil alloy compositions with higher gravimetric hydrogen capacities[70,232], requiring less material to store a given amount of hydrogen and thereby lowering costs.

LOHCs and ammonia offer the distinct advantage of being storable and transportable at ambient temperature in liquid form, thereby

avoiding the extreme conditions required to store hydrogen in its pure form. For LOHCs, efficient hydrogen storage depends on the low ΔH of dehydrogenation. For both LOHCs and ammonia, sustainable, efficient, stable and cost-effective catalysts for synthesis and dehydrogenation under mild conditions must be developed. Furthermore, making green ammonia by carbon-dioxide-free synthesis using renewable energy sources, and developing suitable reactors and catalysts are important to its broader usage. However, political and public acceptance of ammonia will also be crucial to its successful introduction as a hydrogen carrier[127,233,234].

For metal hydride compressors, further material developments should include understanding better how to flatten isotherm plateaus and reduce hysteresis between absorption and desorption isotherms, to improve compression efficiency. Using materials and process informatics, meanwhile, rather than relying simply on trial and error, could accelerate the search for new materials for compression technology. Heat management and high-pressure resistance must be considered to develop systems with high hydrogen flow rates. Improving thermal conductivity using composites should be investigated, as well as designing tanks with internal heat exchange systems. Finally, to enable global distribution of this technology, international standards under ISO-TC197 (for hydrogen technologies) should be established, as they were for transportable hydride tanks, which were standardized as ISO16111 (refs. 235,236).

For electrochemical energy storage, new electrolytes are required for next-generation Ni-MH batteries, together with electrodes based on lightweight Ti, V or Mg hydride-forming alloys, to reduce the use of strategic rare-earth elements. The large structural and compositional diversity of metal hydridoborates has provided the electrolytes, including Li and Na ionic conductors, required for SSBs. New phenomena in the solid state that enhance conductivity allow rational design, synthesis and discovery of high-performance Mg ionic conductors. Current research is exploring other divalent metals such as Ca or Zn. New derivatives of hydrido-*closo*-(car)borates are expected to have higher electrochemical stability. Further efforts could result in unexpected SSBs made of more abundant elements, with higher cell voltages and greater sustainability, with the aim of ultimately superseding current Li-ion battery technology.

Heat storage systems based on metal hydrides are among those with the highest gravimetric thermal energy storage densities. They are potential systems for combining heat storage and hydrogen storage. Depending on the available temperature range, a large number

Box 2 | Sustainability

A critical aspect of the sustainability of hydrogen storage systems is their impact on the environment over their lifetime. Life cycle assessment (LCA) can be used to quantify such impacts[240] and has been widely applied to hydrogen energy systems, particularly different hydrogen production routes[241–243]. LCA has also been performed for various hydrogen storage options[117,244,245], as well as for large-scale, long-distance hydrogen transportation using liquid hydrogen carriers[246,247].

An LCA of metal-hydride-based hydrogen storage, for example, considered the environmental impacts of a storage system for an auxiliary power unit, developed in the framework of the European project SSH2S[244]. When electricity consumption for hydrogen compression was included, solid-state hydrogen storage had similar greenhouse gas emissions and primary energy demand similar to that of type III tanks and type IV tanks. Depletion of resources, however, is higher for the solid-state system, although inclusion of the end-of-life and recycling of materials could lead to different conclusions[244]. In another study, the hydride-based hydrogen storage system developed within the HyCARE project to store about 50 kg of H_2 was found to produce a lower environmental impact than a low pressure (~30 bar) gas storage system, considering the following impact categories: climate change, photochemical ozone formation, particulate matter emissions, acidification, ecotoxicity of freshwater, and resource use of minerals and metals; in the latter case by more than 50%. The impact of the investigated system was shown to be mainly due to its manufacturing process and the associated resources. In comparison, operational life has a relatively small impact, owing to the moderate pressures and temperatures at which metal hydrides operate, which favour long operational life[248].

The materials used affect the system sustainability. Critical raw material use should be minimized, and metal hydride storage systems are moving away from the use of rare-earth elements, such as La, towards Ti, Cr, Mn and similar metals. Titanium is now classified as a critical raw material in the European Union[249–251] and the USA[252], but its production is more diversified than that of rare-earth elements. Environmental impacts and the use of critical raw materials remain open questions for large-scale applications. Ways of reducing environmental impact include increasing weight percentage storage capacities, incorporating thermal energy storage in hydrogen storage systems, and using larger systems in stationary applications[253]. Adopting these approaches, as well as developing systems based on non-critical raw materials, should help to drive the technology towards more sustainable solutions. By contrast, LOHCs can be synthesized from biogenic CO_2. However, emissions from all industrial processes used in growing, harvesting and processing the biogenic feedstock must be considered, in addition to emissions from the hydrogenation and dehydrogenation processes. A total of 7 kg CO_2-equivalent per kg of H_2 was found for ethanol as a liquid carrier[119], similar to emissions from compressed or liquid hydrogen. This impact could be lowered by more efficient recovery of ethanol during cyclic hydrogen storage and release.

Research using LCA has offered valuable insights into MOF sustainability[254–256]. A cradle-to-gate LCA of CPO-27-Ni, for example, found that environmental impact is dominated by solvent use, either in the synthesis or cleaning steps of MOF production[254]. Eliminating organic solvents from the synthesis process led to a nearly hundredfold reduction in CO_2 emissions, and order-of-magnitude reductions in other impact indicators, including freshwater ecotoxicity and resource depletion. Similarly, a cradle-to-gate LCA of ten industrially produced MOFs (including MOF-5, HKUST-1, MOF-74(Mg) and MIL-53), at the kilogram scale and considering 18 environmental impact categories, concluded that the impact of the organic solvent is much higher than the combined impact of all other contributions[256]. Minimizing or eliminating organic solvent use in synthesizing MOFs is therefore critical to reducing the overall environmental impact and hence improving sustainability.

of metal hydrides are available whose suitability has been proved in laboratory tests and smaller demonstration plants. The next step must now be to transfer these results to larger demonstration projects and integrate them into existing production processes, as has already been demonstrated with a heat storage system based on MgH_2.

Published online: 23 June 2026

References

1. Global Hydrogen Review 2025 — analysis. *International Energy Agency* https://www.iea.org/reports/global-hydrogen-review-2025 (2025).
2. Mohtadi, R. & Orimo, S. The renaissance of hydrides as energy materials. *Nat. Rev. Mater.* **2**, 16091 (2016).
3. Eberle, U., Felderhoff, M. & Schüth, F. Chemical and physical solutions for hydrogen storage. *Angew. Chem. Int. Ed.* **48**, 6608–6630 (2009).
4. Broom, D. P. et al. Outlook and challenges for hydrogen storage in nanoporous materials. *Appl. Phys. A* **122**, 151 (2016).
5. Pasquini, L. et al. Magnesium- and intermetallic alloys-based hydrides for energy storage: modelling, synthesis and properties. *Prog. Energy* **4**, 032007 (2022).
6. Orimo, S., Nakamori, Y., Eliseo, J. R., Züttel, A. & Jensen, C. M. Complex hydrides for hydrogen storage. *Chem. Rev.* **107**, 4111–4132 (2007).
7. Milanese, C. et al. Complex hydrides for energy storage. *Int. J. Hydrog. Energy* **44**, 7860–7874 (2019).
8. Dematteis, E. M. et al. Hydrogen storage in complex hydrides: past activities and new trends. *Prog. Energy* **4**, 032009 (2022).
9. Ulucan, T. H. et al. Hydrogen storage in liquid hydrogen carriers: recent activities and new trends. *Prog. Energy* **5**, 012004 (2023).
10. Chen, Z. et al. Balancing volumetric and gravimetric uptake in highly porous materials for clean energy. *Science* **368**, 297–303 (2020).
11. Dornheim, M. et al. Research and development of hydrogen carrier based solutions for hydrogen compression and storage. *Prog. Energy* **4**, 042005 (2022).
12. Yu, Y. et al. Reversible hydrogen uptake/release over a sodium phenoxide–cyclohexanolate pair. *Angew. Chem. Int. Ed.* **58**, 3102–3107 (2019).
13. Fu, X. et al. Continuous-flow electrosynthesis of ammonia by nitrogen reduction and hydrogen oxidation. *Science* **379**, 707–712 (2023).
14. Wu, H. et al. Nitrogen fixation by alkali and alkaline earth metal hydrides assisted by plasma. *Chem. Commun.* **60**, 10760–10763 (2024).
15. Lototskyy, M. V. et al. Modelling of metal hydride hydrogen compressors from thermodynamics of hydrogen–metal interactions viewpoint. Part I. Assessment of the performance of metal hydride materials. *Int. J. Hydrog. Energy* **46**, 2330–2338 (2021).
16. Lototskyy, M. V. et al. Modelling of metal hydride hydrogen compressors from thermodynamics of hydrogen–metal interactions viewpoint. Part II. Assessment of the performance of metal hydride compressors. *Int. J. Hydrog. Energy* **46**, 2339–2350 (2021).
17. Johnson, T. A. et al. Metal hydride compressor for high-pressure (875 bar) hydrogen delivery. *United States Department of Energy Office of Scientific and Technical Information* https://www.osti.gov/biblio/1898257 (2022).
18. Lototskyy, M. V. et al. Development of a high-pressure 700 bar metal hydride hydrogen compressor. *J. Energy Storage* **98**, 113072 (2024).
19. Yan, Y. et al. The mechanism of Mg^{2+} conduction in ammine magnesium borohydride promoted by a neutral molecule. *Phys. Chem. Chem. Phys.* **22**, 9204–9209 (2020).
20. Adams, M. et al. Hydride-based thermal energy storage. *Prog. Energy* **4**, 032008 (2022).
21. Hirscher, M. *Handbook of Hydrogen Storage: New Materials for Future Energy Storage* (Wiley, 2010).
22. Broom, D. P. *Hydrogen Storage Materials: The Characterisation of Their Storage Properties* (Springer, 2011).
23. Ghafri, S. Z. A. et al. Hydrogen liquefaction: a review of the fundamental physics, engineering practice and future opportunities. *Energy Environ. Sci.* **15**, 2690–2731 (2022).
24. Andersson, J. & Grönkvist, S. Large-scale storage of hydrogen. *Int. J. Hydrog. Energy* **44**, 11901–11919 (2019).
25. Stepan, T., Breiteneder, T. & Winklhofer, J. Comparison of liquified gas energy carriers and conventional fossil fuels with a focus on storage requirements for the use in mobile applications. *Salzburger Aluminium Group* https://sag.at/wp-content/uploads/2023/05/sag_whitepaper_comparison_engl.pdf (2023).
26. Lototskyy, M. & Yartys, V. A. Comparative analysis of the efficiencies of hydrogen storage systems utilising solid state H storage materials. *J. Alloys Compd.* **645**, S365–S373 (2015).
27. Chen, Z., Kirlikovali, K. O., Idrees, K. B., Wasson, M. C. & Farha, O. K. Porous materials for hydrogen storage. *Chem* **8**, 693–716 (2022).
28. Bansal, R. C. & Goyal, M. *Activated Carbon Adsorption* (CRC Press, 2005).
29. Carpetis, C. & Peschka, W. A study on hydrogen storage by use of cryoadsorbents. *Int. J. Hydrog. Energy* **5**, 539–554 (1980).
30. Hirscher, M. Hydrogen storage by cryoadsorption in ultrahigh-porosity metal–organic frameworks. *Angew. Chem. Int. Ed.* **50**, 581–582 (2011).
31. Goldsmith, J., Wong-Foy, A. G., Cafarella, M. J. & Siegel, D. J. Theoretical limits of hydrogen storage in metal–organic frameworks: opportunities and trade-offs. *Chem. Mater.* **25**, 3373–3382 (2013).
32. Murray, L. J., Dincă, M. & Long, J. R. Hydrogen storage in metal–organic frameworks. *Chem. Soc. Rev.* **38**, 1294–1314 (2009).
33. Panella, B., Hirscher, M. & Roth, S. Hydrogen adsorption in different carbon nanostructures. *Carbon* **43**, 2209–2214 (2005).
34. Schlichtenmayer, M. & Hirscher, M. Nanosponges for hydrogen storage. *J. Mater. Chem.* **22**, 10134–10143 (2012).
35. Schlichtenmayer, M. & Hirscher, M. The usable capacity of porous materials for hydrogen storage. *Appl. Phys. A* **122**, 379 (2016).
36. Schlichtenmayer, M., Streppel, B. & Hirscher, M. Hydrogen physisorption in high SSA microporous materials — a comparison between AX-21_33 and MOF-177 at cryogenic conditions. *Int. J. Hydrog. Energy* **36**, 586–591 (2011).
37. Broom, D. P. et al. Concepts for improving hydrogen storage in nanoporous materials. *Int. J. Hydrog. Energy* **44**, 7768–7779 (2019).
38. Zhang, R. et al. Balancing volumetric and gravimetric capacity for hydrogen in supramolecular crystals. *Nat. Chem.* **16**, 1982–1988 (2024).
39. Balderas-Xicohténcatl, R., Schlichtenmayer, M. & Hirscher, M. Volumetric hydrogen storage capacity in metal–organic frameworks. *Energy Technol.* **6**, 578–582 (2018).
40. Zhang, L. et al. Fundamentals of hydrogen storage in nanoporous materials. *Prog. Energy* **4**, 042013 (2022).
41. Ahmed, A. et al. Balancing gravimetric and volumetric hydrogen density in MOFs. *Energy Environ. Sci.* **10**, 2459–2471 (2017).
42. Madden, D. G. et al. Densified HKUST-1 monoliths as a route to high volumetric and gravimetric hydrogen storage capacity. *J. Am. Chem. Soc.* **144**, 13729–13739 (2022).
43. Allendorf, M. D. et al. An assessment of strategies for the development of solid-state adsorbents for vehicular hydrogen storage. *Energy Environ. Sci.* **11**, 2784–2812 (2018).
44. Barnett, B. R. et al. Observation of an intermediate to H_2 binding in a metal–organic framework. *J. Am. Chem. Soc.* **143**, 14884–14894 (2021).
45. Allendorf, M. D. et al. Challenges to developing materials for the transport and storage of hydrogen. *Nat. Chem.* **14**, 1214–1223 (2022).
46. Halder, A. et al. Multivariate flexible framework with high usable hydrogen capacity in a reduced pressure swing process. *J. Am. Chem. Soc.* **145**, 8033–8042 (2023).
47. Rowsell, J. L. C. & Yaghi, O. M. Strategies for hydrogen storage in metal–organic frameworks. *Angew. Chem. Int. Ed.* **44**, 4670–4679 (2005).
48. Balderas-Xicohténcatl, R., Schmieder, P., Denysenko, D., Volkmer, D. & Hirscher, M. High volumetric hydrogen storage capacity using interpenetrated metal–organic frameworks. *Energy Technol.* **6**, 510–512 (2018).
49. Nazari, M. et al. Challenges and solutions to the scale-up of porous materials. *Commun. Mater.* **5**, 170 (2024).
50. Wright, A. M., Kapelewski, M. T., Marx, S., Farha, O. K. & Morris, W. Transitioning metal–organic frameworks from the laboratory to market through applied research. *Nat. Mater.* **24**, 178–187 (2025).
51. Broom, D. P. & Hirscher, M. Irreproducibility in hydrogen storage material research. *Energy Environ. Sci.* **9**, 3368–3380 (2016).
52. Broom, D. P. & Hirscher, M. Improving reproducibility in hydrogen storage material research. *ChemPhysChem* **22**, 2141–2157 (2021).
53. Villajos, J. A. et al. Establishing ZIF-8 as a reference material for hydrogen cryoadsorption: an interlaboratory study. *ChemPhysChem* **25**, e202300794 (2024).
54. Balderas-Xicohtencatl, R. et al. ZIF-8 pellets as a robust material for hydrogen cryo-adsorption tanks. *ACS Appl. Energy Mater.* **6**, 9145–9152 (2023).
55. Broom, D. P. Challenges in characterizing adsorbents for gas storage and separation. *Adsorption* **30**, 1565–1591 (2024).
56. Balderas-Xicohténcatl, R. et al. Formation of a super-dense hydrogen monolayer on mesoporous silica. *Nat. Chem.* **14**, 1319–1324 (2022).
57. Oh, H. et al. Small-pore hydridic frameworks store densely packed hydrogen. *Nat. Chem.* **16**, 809–816 (2024).
58. Park, J. et al. 20 K H_2 physisorption on metal–organic frameworks with enhanced dormancy compared to liquid hydrogen storage. *ACS Appl. Energy Mater.* **6**, 9057–9064 (2023).
59. Morales-Ospino, R., Celzard, A. & Fierro, V. Strategies to recover and minimize boil-off losses during liquid hydrogen storage. *Renew. Sustain. Energy Rev.* **182**, 113360 (2023).
60. Bellosta von Colbe, J. et al. Application of hydrides in hydrogen storage and compression: achievements, outlook and perspectives. *Int. J. Hydrog. Energy* **44**, 7780–7808 (2019).
61. Buschow, K. H. J., Bouten, P. C. P. & Miedema, A. R. Hydrides formed from intermetallic compounds of two transition metals: a special class of ternary alloys. *Rep. Prog. Phys.* **45**, 937 (1982).
62. Sandrock, G. A panoramic overview of hydrogen storage alloys from a gas reaction point of view. *J. Alloys Compd.* **293–295**, 877–888 (1999).
63. Züttel, A. Materials for hydrogen storage. *Mater. Today* **6**, 24–33 (2003).
64. Reilly, J. J. & Wiswall, R. H. Formation and properties of iron titanium hydride. *Inorg. Chem.* **13**, 218–222 (1974).
65. Shaltiel, D., Jacob, I. & Davidov, D. Hydrogen absorption and desorption properties of AB_2 Laves-phase pseudobinary compounds. *J. Less Common. Met.* **53**, 117–131 (1977).
66. Van Mal, H. H., Buschow, K. H. J. & Miedema, A. R. Hydrogen absorption in $LaNi_5$ and related compounds: experimental observations and their explanation. *J. Less Common. Met.* **35**, 65–76 (1974).
67. Joubert, J.-M., Paul-Boncour, V., Cuevas, F., Zhang, J. & Latroche, M. $LaNi_5$ related AB_5 compounds: structure, properties and applications. *J. Alloys Compd.* **862**, 158163 (2021).

68. Balcerzak, M. et al. Hydrogen-stabilized ScYNdGd medium-entropy alloy for hydrogen storage. *J. Am. Chem. Soc.* **146**, 5283–5294 (2024).
69. Marques, F., Balcerzak, M., Winkelmann, F., Zepon, G. & Felderhoff, M. Review and outlook on high-entropy alloys for hydrogen storage. *Energy Environ. Sci.* **14**, 5191–5227 (2021).
70. Witman, M. D. et al. Towards Pareto optimal high entropy hydrides via data-driven materials discovery. *J. Mater. Chem. A* **11**, 15878–15888 (2023).
71. Sahlberg, M., Karlsson, D., Zlotea, C. & Jansson, U. Superior hydrogen storage in high entropy alloys. *Sci. Rep.* **6**, 36770 (2016).
72. Montero, J., Ek, G., Sahlberg, M. & Zlotea, C. Improving the hydrogen cycling properties by Mg addition in Ti-V-Zr-Nb refractory high entropy alloy. *Scr. Mater.* **194**, 113699 (2021).
73. Li, X. et al. Magnesium borohydride $Mg(BH_4)_2$ for energy applications: a review. *J. Mater. Sci. Technol.* **161**, 170–179 (2023).
74. Patelli, N., Migliori, A., Morandi, V. & Pasquini, L. Interfaces within biphasic nanoparticles give a boost to magnesium-based hydrogen storage. *Nano Energy* **72**, 104654 (2020).
75. Dematteis, E. M., Berti, N., Cuevas, F., Latroche, M. & Baricco, M. Substitutional effects in TiFe for hydrogen storage: a comprehensive review. *Mater. Adv.* **2**, 2524–2560 (2021).
76. Bogdanović, B. & Schwickardi, M. Ti-doped alkali metal aluminium hydrides as potential novel reversible hydrogen storage materials. *J. Alloys Compd.* **253–254**, 1–9 (1997).
77. Bellosta von Colbe, J. M. et al. Design, sorption behaviour and energy management in a sodium alanate-based lightweight hydrogen storage tank. *Int. J. Hydrog. Energy* **40**, 2984–2988 (2015).
78. Barkhordarian, G., Klassen, T., Dornheim, M. & Bormann, R. Unexpected kinetic effect of MgB_2 in reactive hydride composites containing complex borohydrides. *J. Alloys Compd.* **440**, L18–L21 (2007).
79. Bösenberg, U. et al. Role of additives in $LiBH_4$–MgH_2 reactive hydride composites for sorption kinetics. *Acta Mater.* **58**, 3381–3389 (2010).
80. Schneemann, A. et al. Nanostructured metal hydrides for hydrogen storage. *Chem. Rev.* **118**, 10775–10839 (2018).
81. Stavila, V. et al. Defying thermodynamics: stabilization of alane within covalent triazine frameworks for reversible hydrogen storage. *Angew. Chem. Int. Ed.* **60**, 25815–25824 (2021).
82. Cho, Y. et al. Reversing the irreversible: thermodynamic stabilization of $LiAlH_4$ nanoconfined within a nitrogen-doped carbon host. *ACS Nano* **15**, 10163–10174 (2021).
83. Crivello, J.-C. et al. Review of magnesium hydride-based materials: development and optimisation. *Appl. Phys. A* **122**, 97 (2016).
84. Yartys, V. A. et al. Magnesium based materials for hydrogen based energy storage: past, present and future. *Int. J. Hydrog. Energy* **44**, 7809–7859 (2019).
85. Severa, G., Rönnebro, E. & Jensen, C. M. Direct hydrogenation of magnesium boride to magnesium borohydride: demonstration of >11 weight percent reversible hydrogen storage. *Chem. Commun.* **46**, 421–423 (2010).
86. Wood, B. C., Heo, T. W., Kang, S., Wan, L. F. & Li, S. Beyond idealized models of nanoscale metal hydrides for hydrogen storage. *Ind. Eng. Chem. Res.* **59**, 5786–5796 (2020).
87. Alvares, E. et al. Multiscale modeling of metal-hydride interphases — quantification of decoupled chemo-mechanical energies. *npj Comput. Mater.* **10**, 249 (2024).
88. Moran, C., Deane, P., Yousefian, S. & Monaghan, R. F. D. The hydrogen storage challenge: does storage method and size affect the cost and operational flexibility of hydrogen supply chains? *Int. J. Hydrog. Energy* **52**, 1090–1100 (2024).
89. Wang, X. et al. Technoeconomic insights into metal hydrides for stationary hydrogen storage. *Adv. Sci.* **12**, 2415736 (2025).
90. Mehr, A. S., Phillips, A. D., Brandon, M. P., Pryce, M. T. & Carton, J. G. Recent challenges and development of technical and technoeconomic aspects for hydrogen storage, insights at different scales; a state of art review. *Int. J. Hydrog. Energy* **70**, 786–815 (2024).
91. Shang, Y. et al. Developing sustainable FeTi alloys for hydrogen storage by recycling. *Commun. Mater.* **3**, 101 (2022).
92. Ugaddan, E. et al. AB_5-based metal hydride embedded in polyethylene and polymethylmethacrylate for hydrogen storage. *Int. J. Hydrog. Energy* **78**, 952–961 (2024).
93. Witman, M. D. et al. A bulk versus nanoscale hydrogen storage paradox revealed by material–system co-design. *Adv. Funct. Mater.* **34**, 2411763 (2024).
94. Barale, J. et al. $TiFe_{0.85}Mn_{0.05}$ alloy produced at industrial level for a hydrogen storage plant. *Int. J. Hydrog. Energy* **47**, 29866–29880 (2022).
95. Dreistadt, D. M. et al. An effective activation method for industrially produced TiFeMn powder for hydrogen storage. *J. Alloys Compd.* **919**, 165847 (2022).
96. Dreistadt, D. M. et al. A novel emergency gas-to-power system based on an efficient and long-lasting solid-state hydride storage system: modeling and experimental validation. *Energies* **15**, 844 (2022).
97. Messa, A. R. et al. Risk management in a containerized metal hydride storage system. *Hydrog. Saf.* **1**, 33–45 (2024).
98. Puszkiel, J. et al. Designing an AB_2-type alloy (TiZr-CrMnMo) for the hybrid hydrogen storage concept. *Energies* **13**, 2751 (2020).
99. Adams, M. J., Wadge, M. D., Sheppard, D., Stuart, A. & Grant, D. M. Review on onshore and offshore large-scale seasonal hydrogen storage for electricity generation: focusing on improving compression, storage, and roundtrip efficiency. *Int. J. Hydrog. Energy* **73**, 95–111 (2024).
100. Lototskyy, M. et al. Metal hydride hydrogen storage tank for fuel cell utility vehicles. *Int. J. Hydrog. Energy* **45**, 7958–7967 (2020).
101. Ye, J. et al. Optimization design of solid-state hydrogen storage device for fuel cell forklift. *J. Alloys Compd.* **970**, 172242 (2024).
102. Krummrich, S. & Hammerschmidt, A. in *Hydrogen Science and Engineering: Materials, Processes, Systems and Technology* (eds Stolten, D. & Emonts, B.) Ch. 42 (Wiley, 2016).
103. Kapetanović, M., Núñez, A., van Oort, N. & Goverde, R. M. P. Analysis of hydrogen-powered propulsion system alternatives for diesel-electric regional trains. *J. Rail Transp. Plan. Manag.* **23**, 100338 (2022).
104. Danebergs, J. & Deledda, S. Can hydrogen storage in metal hydrides be economically competitive with compressed and liquid hydrogen storage? A techno-economical perspective for the maritime sector. *Int. J. Hydrog. Energy* **50**, 1040–1054 (2024).
105. Lin, X. et al. A one- and three-dimensional coupled model and simulation investigation for the large-scale oil-heating type Mg-based hydrogen storage tank. *Chem. Eng. J.* **472**, 144943 (2023).
106. Valenzuela-Venegas, G. et al. A renewable and socially accepted energy system for astronomical telescopes. *Nat. Sustain.* **7**, 1642–1650 (2024).
107. Viole, I., Valenzuela-Venegas, G., Zeyringer, M. & Sartori, S. A renewable power system for an off-grid sustainable telescope fueled by solar power, batteries and green hydrogen. *Energy* **282**, 128570 (2023).
108. Preuster, P., Papp, C. & Wasserscheid, P. Liquid organic hydrogen carriers (LOHCs): toward a hydrogen-free hydrogen economy. *Acc. Chem. Res.* **50**, 74–85 (2017).
109. Okada, Y., Sasaki, E., Watanabe, E., Hyodo, S. & Nishijima, H. Development of dehydrogenation catalyst for hydrogen generation in organic chemical hydride method. *Int. J. Hydrog. Energy* **31**, 1348–1356 (2006).
110. Jorschick, H. et al. Hydrogen storage using a hot pressure swing reactor. *Energy Environ. Sci.* **10**, 1652–1659 (2017).
111. Tran, B. L., Johnson, S. I., Brooks, K. P. & Autrey, S. T. Ethanol as a liquid organic hydrogen carrier for seasonal microgrid application: catalysis, theory, and engineering feasibility. *ACS Sustain. Chem. Eng.* **9**, 7130–7138 (2021).
112. Grubel, K., Jeong, H., Yoon, C. W. & Autrey, T. Challenges and opportunities for using formate to store, transport, and use hydrogen. *J. Energy Chem.* **41**, 216–224 (2020).
113. Aakko-Saksa, P. T., Cook, C., Kiviaho, J. & Repo, T. Liquid organic hydrogen carriers for transportation and storing of renewable energy — review and discussion. *J. Power Sources* **396**, 803–823 (2018).
114. Le, T.-H., Tran, N. & Lee, H.-J. Development of liquid organic hydrogen carriers for hydrogen storage and transport. *Int. J. Mol. Sci.* **25**, 1359 (2024).
115. Crabtree, R. H. Nitrogen-containing liquid organic hydrogen carriers: progress and prospects. *ACS Sustain. Chem. Eng.* **5**, 4491–4498 (2017).
116. Stark, K. et al. Liquid organic hydrogen carriers: thermophysical and thermochemical studies of carbazole partly and fully hydrogenated derivatives. *Ind. Eng. Chem. Res.* **54**, 7953–7966 (2015).
117. Mevawala, C. et al. The ethanol–ethyl acetate system as a biogenic hydrogen carrier. *Energy Technol.* **11**, 2200892 (2023).
118. Niermann, M., Beckendorff, A., Kaltschmitt, M. & Bonhoff, K. Liquid organic hydrogen carrier (LOHC) — assessment based on chemical and economic properties. *Int. J. Hydrog. Energy* **44**, 6631–6654 (2019).
119. Mevawala, C. et al. 1,4-Butanediol as a hydrogen carrier: liquid- versus gas-phase dehydrogenation. *Energy Fuels* **37**, 560–566 (2023).
120. Gutiérrez, O. Y. et al. Using earth abundant materials for long duration energy storage: electro-chemical and thermo-chemical cycling of bicarbonate/formate. *Green Chem.* **25**, 4222–4233 (2023).
121. Grubel, K. et al. Research requirements to move the bar forward using aqueous formate salts as H_2 carriers for energy storage applications. *J. Energy Power Technol.* **2**, 1–21 (2020).
122. Shyong, J., Bowden, M., Autrey, T., Saqline, S. & Breunig, H. Technoeconomic analysis of hydrogen storage using 1,4-butanediol (BDO)/γ-butyrolactone (GBL) as a stationary backup power system. *Int. J. Hydrog. Energy* **208**, 153161 (2026).
123. Jorschick, H., Vogl, M., Preuster, P., Bösmann, A. & Wasserscheid, P. Hydrogenation of liquid organic hydrogen carrier systems using multicomponent gas mixtures. *Int. J. Hydrog. Energy* **44**, 31172–31182 (2019).
124. Chen, Y. et al. A catalytic cycle that enables crude hydrogen separation, storage and transportation. *Nat. Energy* **10**, 971–980 (2025).
125. Valera-Medina, A., Xiao, H., Owen-Jones, M., David, W. I. F. & Bowen, P. J. Ammonia for power. *Prog. Energy Combust. Sci.* **69**, 63–102 (2018).
126. Kyriakou, V., Garagounis, I., Vourros, A., Vasileiou, E. & Stoukides, M. An electrochemical Haber–Bosch process. *Joule* **4**, 142–158 (2020).
127. MacFarlane, D. R. et al. A roadmap to the ammonia economy. *Joule* **4**, 1186–1205 (2020).
128. Khalid, H. et al. Technical, economic, and environmental optimization of the renewable hydrogen production chain for use in ammonia production: a case study. *Processes* **13**, 2211 (2025).
129. Zhang, W. et al. New technologies reduce greenhouse gas emissions from nitrogenous fertilizer in China. *Proc. Natl Acad. Sci. USA* **110**, 8375–8380 (2013).
130. Ammonia technology roadmap — analysis. *International Energy Agency* https://www.iea.org/reports/ammonia-technology-roadmap (2021).
131. Hatzell, M. C. The colors of ammonia. *ACS Energy Lett.* **9**, 2920–2921 (2024).
132. Wang, L. et al. Greening ammonia toward the solar ammonia refinery. *Joule* **2**, 1055–1074 (2018).
133. Suryanto, B. H. R. et al. Nitrogen reduction to ammonia at high efficiency and rates based on a phosphonium proton shuttle. *Science* **372**, 1187–1191 (2021).
134. Guo, J. & Chen, P. Interplay of alkali, transition metals, nitrogen, and hydrogen in ammonia synthesis and decomposition reactions. *Acc. Chem. Res.* **54**, 2434–2444 (2021).
135. Guan, Y. et al. Barium chromium nitride-hydride for ammonia synthesis. *Chem. Catal.* **1**, 1042–1054 (2021).

136. Wang, Q. et al. Ternary ruthenium complex hydrides for ammonia synthesis via the associative mechanism. *Nat. Catal.* **4**, 959–967 (2021).
137. Chang, F. et al. Potassium hydride-intercalated graphite as an efficient heterogeneous catalyst for ammonia synthesis. *Nat. Catal.* **5**, 222–230 (2022).
138. Hagen, A., Caldogno, R. & Sun, X. Direct ammonia SOFC — a potential technology for green shipping. *Fuel* **365**, 131238 (2024).
139. Wan, Z., Tao, Y., Shao, J., Zhang, Y. & You, H. Ammonia as an effective hydrogen carrier and a clean fuel for solid oxide fuel cells. *Energy Convers. Manag.* **228**, 113729 (2021).
140. Cechetto, V., Anello, G., Rahimalimamaghani, A. & Gallucci, F. Carbon molecular sieve membrane reactors for ammonia cracking. *Processes* **12**, 1168 (2024).
141. Sitar, R. et al. Compact ammonia reforming at low temperature using catalytic membrane reactors. *J. Membr. Sci.* **644**, 120147 (2022).
142. Lucentini, I., Garcia, X., Vendrell, X. & Llorca, J. Review of the decomposition of ammonia to generate hydrogen. *Ind. Eng. Chem. Res.* **60**, 18560–18611 (2021).
143. Vitse, F., Cooper, M. & Botte, G. G. On the use of ammonia electrolysis for hydrogen production. *J. Power Sources* **142**, 18–26 (2005).
144. Yang, Y. et al. A rigorous electrochemical ammonia electrolysis protocol with *in operando* quantitative analysis. *J. Mater. Chem. A* **9**, 11571–11579 (2021).
145. Nguyen, T. N., Doan, T. L. & Kim, T. A review of recent progress and future perspectives in catalyst design for the electrocatalytic ammonia oxidation reaction. *J. Power Sources* **663**, 238907 (2026).
146. Tseng, J.-C. et al. Tracking the active catalyst for iron-based ammonia decomposition by *in situ* synchrotron diffraction studies. *ChemCatChem* **10**, 4465–4472 (2018).
147. Weidenthaler, C. et al. In-situ investigations of Co@Al_2O_3 ammonia decomposition catalysts: the interaction between support and catalyst. *ChemCatChem* **14**, e202200688 (2022).
148. Gallus, S. & Weidenthaler, C. Systematic *in situ* investigation of the formation of NH_3 cracking catalysts from precursor perovskites ABO_3 (A=La,Ca,Sr and B=Fe,Co,Ni) and their catalytic performance. *ChemCatChem* **15**, e202300947 (2023).
149. Ulucan, T. H. et al. Unveiling the structure–property relationship of MgO-supported Ni ammonia decomposition catalysts from bulk to atomic structure by in situ/operando studies. *ACS Catal.* **14**, 2828–2841 (2024).
150. Lototskyy, M. V., Yartys, V. A., Pollet, B. G. & Bowman, R. C. Metal hydride hydrogen compressors: a review. *Int. J. Hydrog. Energy* **39**, 5818–5851 (2014).
151. Yartys, V. A. et al. Metal hydride hydrogen compression: recent advances and future prospects. *Appl. Phys. A* **122**, 415 (2016).
152. Sdanghi, G., Maranzana, G., Celzard, A. & Fierro, V. Review of the current technologies and performances of hydrogen compression for stationary and automotive applications. *Renew. Sustain. Energy Rev.* **102**, 150–170 (2019).
153. Arjomand Kermani, N., Petrushina, I. & Rokni, M. M. Evaluation of ionic liquids as replacements for the solid piston in conventional hydrogen reciprocating compressors: a review. *Int. J. Hydrog. Energy* **45**, 16337–16354 (2020).
154. Grigoriev, S. A., Shtatniy, I. G., Millet, P., Porembsky, V. I. & Fateev, V. N. Description and characterization of an electrochemical hydrogen compressor/concentrator based on solid polymer electrolyte technology. *Int. J. Hydrog. Energy* **36**, 4148–4155 (2011).
155. Peng, Z. et al. Overview of hydrogen compression materials based on a three-stage metal hydride hydrogen compressor. *J. Alloys Compd.* **895**, 162465 (2022).
156. Cousins, A. et al. Alloy selection for dual stage metal-hydride hydrogen compressor: using a thermodynamic model to identify metal-hydride pairs. *Int. J. Hydrog. Energy* **48**, 28453–28459 (2023).
157. Zohra, F. T., Webb, C. J., Lamb, K. E. & Gray, E. MacA. Degradation of metal hydrides in hydrogen-based thermodynamic machines: a review. *Int. J. Hydrog. Energy* **64**, 417–438 (2024).
158. Charbonnier, V., Enoki, H., Asano, K., Kim, H. & Sakaki, K. Tuning the hydrogenation properties of $Ti_{1+y}Cr_{2-x}Mn_x$ Laves phase compounds for high pressure metal-hydride compressors. *Int. J. Hydrog. Energy* **46**, 36369–36380 (2021).
159. Smith, D. B., Bowman, R. C., Anovitz, L. M., Corgnale, C. & Sulic, M. Isotherm measurements of high-pressure metal hydrides for hydrogen compressors. *J. Phys. Energy* **3**, 034004 (2021).
160. Broom, D. P. & Webb, C. J. Pitfalls in the characterisation of the hydrogen sorption properties of materials. *Int. J. Hydrog. Energy* **42**, 29320–29343 (2017).
161. Charbonnier, V., Asano, K., Kim, H. & Sakaki, K. How to evaluate hydrogen storage properties by Sieverts' method in the pressure range up to 100 MPa. *J. Alloys Compd.* **960**, 170860 (2023).
162. Beeri, O., Cohen, D., Gavra, Z., Johnson, J. R. & Mintz, M. H. Thermodynamic characterization and statistical thermodynamics of the TiCrMn–$H_2(D_2)$ system. *J. Alloys Compd.* **299**, 217–226 (2000).
163. Stamatakis, E. et al. Metal hydride hydrogen compressors: current developments & early markets. *Renew. Energy* **127**, 850–862 (2018).
164. Chahrouri, R., Colomar, D., Jeanmougin, A. & Martinez-Abenojar, A. The COSMHYC project series: innovative hydrogen compression solutions. *Chem. Ing. Tech.* **96**, 36–42 (2024).
165. Corgnale, C. et al. Technical performance of a hybrid thermo-electrochemical system for high pressure hydrogen compression. *ECS Trans.* **80**, 41 (2017).
166. Cuevas, F., Joubert, J.-M., Latroche, M. & Percheron-Guégan, A. Intermetallic compounds as negative electrodes of Ni/MH batteries. *Appl. Phys. A* **72**, 225–238 (2001).
167. Fetcenko, M. A. et al. Recent advances in NiMH battery technology. *J. Power Sources* **165**, 544–551 (2007).
168. Taniguchi, A., Fujioka, N., Ikoma, M. & Ohta, A. Development of nickel/metal-hydride batteries for EVs and HEVs. *J. Power Sources* **100**, 117–124 (2001).
169. Armand, M. & Tarascon, J.-M. Building better batteries. *Nature* **451**, 652–657 (2008).
170. Famprikis, T., Canepa, P., Dawson, J. A., Islam, M. S. & Masquelier, C. Fundamentals of inorganic solid-state electrolytes for batteries. *Nat. Mater.* **18**, 1278–1291 (2019).
171. Goodenough, J. B. & Kim, Y. Challenges for rechargeable Li batteries. *Chem. Mater.* **22**, 587–603 (2010).
172. Monnier, J., Zhang, J., Paul-Boncour, V. & Cuevas, F. in *Corrosion and Degradation in Fuel Cells, Supercapacitors and Batteries* (ed. Saji, V. S.) 219–249 (Springer Nature, 2024).
173. Cuevas, F. et al. Metallic and complex hydride-based electrochemical storage of energy. *Prog. Energy* **4**, 032001 (2022).
174. Kohno, T. et al. Hydrogen storage properties of new ternary system alloys: La_2MgNi_9, $La_5Mg_2Ni_{23}$, La_3MgNi_{14}. *J. Alloys Compd.* **311**, L5–L7 (2000).
175. Meng, T., Young, K.-H., Wong, D. F. & Nei, J. Ionic liquid-based non-aqueous electrolytes for nickel/metal hydride batteries. *Batteries* **3**, 4 (2017).
176. Chaabene, N. et al. Toward new proton exchange batteries based on ionic liquid electrolyte: metal hydride electrode/electrolyte coupling. *J. Power Sources* **574**, 233176 (2023).
177. El Kharbachi, A. et al. Exploits, advances and challenges benefiting beyond Li-ion battery technologies. *J. Alloys Compd.* **817**, 153261 (2020).
178. Pasta, M. et al. 2020 roadmap on solid-state batteries. *J. Phys. Energy* **2**, 032008 (2020).
179. Palacin, M. R. et al. Roadmap on multivalent batteries. *J. Phys. Energy* **6**, 031501 (2024).
180. Unemoto, A., Matsuo, M. & Orimo, S. Complex hydrides for electrochemical energy storage. *Adv. Funct. Mater.* **24**, 2267–2279 (2014).
181. Mohtadi, R. Beyond typical electrolytes for energy dense batteries. *Molecules* **25**, 1791 (2020).
182. Janek, J. & Zeier, W. G. Challenges in speeding up solid-state battery development. *Nat. Energy* **8**, 230–240 (2023).
183. Kisu, K. et al. Magnesium borohydride ammonia borane as a magnesium ionic conductor. *ACS Appl. Energy Mater.* **3**, 3174–3179 (2020).
184. Černý, R., Murgia, F. & Brighi, M. Metal hydroborates: from hydrogen stores to solid electrolytes. *J. Alloys Compd.* **895**, 162659 (2022).
185. Grinderslev, J. B. et al. New perspectives of functional metal borohydrides. *J. Alloys Compd.* **896**, 163014 (2022).
186. Paskevicius, M. et al. Metal borohydrides and derivatives — synthesis, structure and properties. *Chem. Soc. Rev.* **46**, 1565–1634 (2017).
187. Skov, L. N., Grinderslev, J. B. & Jensen, T. R. Layered titanium sulfide cathode for all-solid-state magnesium batteries. *Batt. Supercaps* **6**, e202300185 (2023).
188. Skov, L. N., Grinderslev, J. B., Rosenkranz, A., Lee, Y.-S. & Jensen, T. R. Towards solid-state magnesium batteries: ligand-assisted superionic conductivity. *Batt. Supercaps* **5**, e202200163 (2022).
189. Skov, L. N., Grinderslev, J. B., Kjær, T. S. S., Kristensen, L. R. & Jensen, T. R. Towards solid-state batteries using a calcium hydridoborate electrolyte. *Angew. Chem. Int. Ed.* **64**, e202500613 (2025).
190. Berger, A., Buckley, C. E. & Paskevicius, M. Synthesis of *closo*-$CB_{11}H_{12}^-$ salts using common laboratory reagents. *Inorg. Chem.* **60**, 14744–14751 (2021).
191. Grinderslev, J. B. et al. Polymorphism and solid solutions of trimethylammonium monocarboranes. *Dalton Trans.* **51**, 15806–15815 (2022).
192. Kristensen, L. R., Herrmann, G. J., Skibsted, J. & Jensen, T. R. Effect of mechanical pressure on the ionic conductivity of sodium dodecahydrido-*closo*-dodecaborate. *ACS Mater. Lett.* **7**, 990–995 (2025).
193. Asakura, R. et al. 4 V room-temperature all-solid-state sodium battery enabled by a passivating cathode/hydroborate solid electrolyte interface. *Energy Environ. Sci.* **13**, 5048–5058 (2020).
194. Mohtadi, R., Matsui, M., Arthur, T. S. & Hwang, S.-J. Magnesium borohydride: from hydrogen storage to magnesium battery. *Angew. Chem. Int. Ed.* **51**, 9780–9783 (2012).
195. Tutusaus, O. et al. An efficient halogen-free electrolyte for use in rechargeable magnesium batteries. *Angew. Chem. Int. Ed.* **54**, 7900–7904 (2015).
196. Dong, H. et al. High-power Mg batteries enabled by heterogeneous enolization redox chemistry and weakly coordinating electrolytes. *Nat. Energy* **5**, 1043–1050 (2020).
197. Mohtadi, R., Tutusaus, O., Arthur, T. S., Zhao-Karger, Z. & Fichtner, M. The metamorphosis of rechargeable magnesium batteries. *Joule* **5**, 581–617 (2021).
198. Kisu, K. et al. Monocarborane cluster as a stable fluorine-free calcium battery electrolyte. *Sci. Rep.* **11**, 7563 (2021).
199. Kisu, K., Mohtadi, R. & Orimo, S. Calcium metal batteries with long cycle life using a hydride-based electrolyte and copper sulfide electrode. *Adv. Sci.* **10**, 2301178 (2023).
200. Green, M. et al. *Closo*-borate gel polymer electrolyte with remarkable electrochemical stability and a wide operating temperature window. *Adv. Sci.* **9**, 2106032 (2022).
201. Shinohara, T. et al. Complex hydride-based gel polymer electrolytes for rechargeable Ca-metal batteries. *Adv. Sci.* **11**, 2308318 (2024).
202. Henry, A., Prasher, R. & Majumdar, A. Five thermal energy grand challenges for decarbonization. *Nat. Energy* **5**, 635–637 (2020).
203. Thiel, G. P. & Stark, A. K. To decarbonize industry, we must decarbonize heat. *Joule* **5**, 531–550 (2021).
204. Forman, C., Muritala, I. K., Pardemann, R. & Meyer, B. Estimating the global waste heat potential. *Renew. Sustain. Energy Rev.* **57**, 1568–1579 (2016).
205. Firth, A., Zhang, B. & Yang, A. Quantification of global waste heat and its environmental effects. *Appl. Energy* **235**, 1314–1334 (2019).
206. Zhao, Y., Zhao, C. Y., Markides, C. N., Wang, H. & Li, W. Medium- and high-temperature latent and thermochemical heat storage using metals and metallic compounds as heat storage media: a technical review. *Appl. Energy* **280**, 115950 (2020).

207. Romero, M. & Steinfeld, A. Concentrating solar thermal power and thermochemical fuels. *Energy Environ. Sci.* **5**, 9234–9245 (2012).
208. Liu, M. et al. Review on concentrating solar power plants and new developments in high temperature thermal energy storage technologies. *Renew. Sustain. Energy Rev.* **53**, 1411–1432 (2016).
209. Aftab, W. et al. Phase change material-integrated latent heat storage systems for sustainable energy solutions. *Energy Environ. Sci.* **14**, 4268–4291 (2021).
210. Gil, A. et al. State of the art on high temperature thermal energy storage for power generation. Part 1 — concepts, materials and modellization. *Renew. Sustain. Energy Rev.* **14**, 31–55 (2010).
211. Carrillo, A. J., González-Aguilar, J., Romero, M. & Coronado, J. M. Solar energy on demand: a review on high temperature thermochemical heat storage systems and materials. *Chem. Rev.* **119**, 4777–4816 (2019).
212. Manickam, K. et al. Future perspectives of thermal energy storage with metal hydrides. *Int. J. Hydrog. Energy* **44**, 7738–7745 (2019).
213. Felderhoff, M., Urbanczyk, R. & Peil, S. Thermochemical heat storage for high temperature applications — a review. *Green* **3**, 113–123 (2013).
214. Felderhoff, M. & Bogdanović, B. High temperature metal hydrides as heat storage materials for solar and related applications. *Int. J. Mol. Sci.* **10**, 325–344 (2009).
215. Sheppard, D. A. et al. Hydriding characteristics of $NaMgH_2F$ with preliminary technical and cost evaluation of magnesium-based metal hydride materials for concentrating solar power thermal storage. *RSC Adv.* **4**, 26552–26562 (2014).
216. Corgnale, C. et al. Screening analysis of metal hydride based thermal energy storage systems for concentrating solar power plants. *Renew. Sustain. Energy Rev.* **38**, 821–833 (2014).
217. Feng, P. et al. Techno-economic analysis of screening metal hydride pairs for a 910 MWh_{th} thermal energy storage system. *Appl. Energy* **242**, 148–156 (2019).
218. Bogdanović, B., Ritter, A. & Spliethoff, B. Active MgH_2–Mg systems for reversible chemical energy storage. *Angew. Chem. Int. Ed. Engl.* **29**, 223–234 (1990).
219. Albert, R., Wagner, C., Urbanczyk, R. & Felderhoff, M. Effective thermal conductivity of dimagnesium iron hexahydride (Mg_2FeH_6) for heat storage applications. *Appl. Phys. A* **129**, 62 (2022).
220. Humphries, T. D., Sheppard, D. A., Rowles, M. R., Sofianos, M. V. & Buckley, C. E. Fluoride substitution in sodium hydride for thermal energy storage applications. *J. Mater. Chem. A* **4**, 12170–12178 (2016).
221. Humphries, T. D. et al. Physicochemical characterization of a Na–H–F thermal battery material. *J. Phys. Chem. C* **124**, 5053–5060 (2020).
222. Tortoza, M. S. et al. Thermodynamics and performance of the Mg–H–F system for thermochemical energy storage applications. *Phys. Chem. Chem. Phys.* **20**, 2274–2283 (2018).
223. Humphries, T. D. et al. Fluorine substitution in magnesium hydride as a tool for thermodynamic control. *J. Phys. Chem. C* **124**, 9109–9117 (2020).
224. Balakrishnan, S., Humphries, T. D., Paskevicius, M. & Buckley, C. E. Thermodynamic and kinetic properties of calcium hydride. *Int. J. Hydrog. Energy* **48**, 30479–30488 (2023).
225. Ward, P. A., Teprovich, J. A., Liu, Y., He, J. & Zidan, R. High temperature thermal energy storage in the $CaAl_2$ system. *J. Alloys Compd.* **735**, 2611–2615 (2018).
226. Desage, L., Humphries, T. D., Paskevicius, M. & Buckley, C. E. Calcium hydride with aluminium for thermochemical energy storage applications. *Sustain. Energy Fuels* **8**, 142–149 (2023).
227. Sofianos, M. V. et al. Exploring halide destabilised calcium hydride as a high-temperature thermal battery. *J. Alloys Compd.* **819**, 153340 (2020).
228. Balakrishnan, S., Sofianos, M. V., Paskevicius, M., Rowles, M. R. & Buckley, C. E. Destabilized calcium hydride as a promising high-temperature thermal battery. *J. Phys. Chem. C* **124**, 17512–17519 (2020).
229. Balakrishnan, S., Sofianos, M. V., Humphries, T. D., Paskevicius, M. & Buckley, C. E. Thermochemical energy storage performance of zinc destabilized calcium hydride at high-temperatures. *Phys. Chem. Chem. Phys.* **22**, 25780–25788 (2020).
230. Griffond, A. C. M. et al. High-temperature thermochemical energy storage using metal hydrides: destabilisation of calcium hydride with silicon. *J. Alloys Compd.* **858**, 158229 (2021).
231. Poupin, L., Humphries, T. D., Paskevicius, M. & Buckley, C. E. A thermal energy storage prototype using sodium magnesium hydride. *Sustain. Energy Fuels* **3**, 985–995 (2019).
232. Jang, S.-H. et al. Physically interpretable descriptors drive the materials design of metal hydrides for hydrogen storage. *Chem. Sci.* **16**, 23111–23120 (2025).
233. Guati-Rojo, A., Demski, C., Poortinga, W. & Valera-Medina, A. Public attitudes and concerns about ammonia as an energy vector. *Energies* **14**, 7296 (2021).
234. Park, Y., Park, S. Y. & Lee, H. Consumers' acceptance of the explosion, toxicity, and odor potential of ammonia: a survey on consumers' choice of an ammonia-based hydrogen refueling station. *Sustain. Energy Technol. Assess.* **58**, 103374 (2023).
235. ISO 16111:2018 Transportable gas storage devices — hydrogen absorbed in reversible metal hydride. *International Organization for Standardization* https://www.iso.org/standard/67952.html (2018).
236. Haloua, F., Bacquart, T., Arrhenius, K., Delobelle, B. & Ent, H. Metrology for hydrogen energy applications: a project to address normative requirements. *Meas. Sci. Technol.* **29**, 034001 (2018).
237. Bogdanović, B., Brand, R. A., Marjanović, A., Schwickardi, M. & Tölle, J. Metal-doped sodium aluminium hydrides as potential new hydrogen storage materials. *J. Alloys Compd.* **302**, 36–58 (2000).
238. Dematteis, E. M. et al. Fundamental hydrogen storage properties of TiFe-alloy with partial substitution of Fe by Ti and Mn. *J. Alloys Compd.* **874**, 159925 (2021).
239. Guo, J. & Chen, P. Ammonia history in the making. *Nat. Catal.* **4**, 734–735 (2021).
240. *Handbook on Life Cycle Sustainability Assessment* (eds Valdivia, S. & Sonnemann, G.) (Edward Elgar, 2024).
241. Valente, A., Iribarren, D. & Dufour, J. Life cycle assessment of hydrogen energy systems: a review of methodological choices. *Int. J. Life Cycle Assess.* **22**, 346–363 (2017).
242. Valente, A., Iribarren, D. & Dufour, J. Harmonised life-cycle global warming impact of renewable hydrogen. *J. Clean. Prod.* **149**, 762–772 (2017).
243. Hren, R. et al. Hydrogen production, storage and transport for renewable energy and chemicals: an environmental footprint assessment. *Renew. Sustain. Energy Rev.* **173**, 113113 (2023).
244. Agostini, A. et al. Role of hydrogen tanks in the life cycle assessment of fuel cell-based auxiliary power units. *Appl. Energy* **215**, 1–12 (2018).
245. Viole, I., Shen, L., Camargo, L. R., Zeyringer, M. & Sartori, S. Sustainable astronomy: a comparative life cycle assessment of off-grid hybrid energy systems to supply large telescopes. *Int. J. Life Cycle Assess.* **29**, 1706–1726 (2024).
246. Bano, S., Siluvai Antony, P., Jangde, V. & Biniwale, R. B. Hydrogen transportation using liquid organic hydrides: a comprehensive life cycle assessment. *J. Clean. Prod.* **183**, 988–997 (2018).
247. Arrigoni, A. et al. *Environmental Life Cycle Assessment (LCA) Comparison of Hydrogen Delivery Options within Europe* (Publications Office of the European Union, 2024).
248. Alves, E. S. et al. Life cycle assessment for the determination of the environmental impacts of an advanced large-scale hydrogen storage system from HyCARE EU project. *J. Clean. Prod.* **515**, 145836 (2025).
249. Jakimów, M., Samokhalov, V. & Baldassarre, B. Achieving European Union strategic autonomy: circularity in critical raw materials value chains. *Int. Aff.* **100**, 1735–1748 (2024).
250. Buesa, A., Piñero, P., Pedauga, L., Rueda-Cantuche, J. M. & Baldassarre, B. The benefits of enhanced circularity on strategic autonomy: titanium metal in the EU. *Resour. Policy* **111**, 105793 (2025).
251. van Gaalen, J. M. & Chris Slootweg, J. From critical raw materials to circular raw materials. *ChemSusChem* **18**, e202401170 (2025).
252. Iyer, R. K. & Kelly, J. C. Life-cycle inventory of critical materials: nickel, copper, titanium, and rare-earth elements. *Argonne National Laboratory* https://publications.anl.gov/anlpubs/2022/12/178670.pdf (2022).
253. Alves, E. et al. Life cycle assessments in hydrogen-based energy storage systems. *J. Energy Storage* **133**, 118008 (2025).
254. Grande, C. A., Blom, R., Spjelkavik, A., Moreau, V. & Payet, J. Life-cycle assessment as a tool for eco-design of metal-organic frameworks (MOFs). *Sustain. Mater. Technol.* **14**, 11–18 (2017).
255. Escobar-Hernandez, H. U., Quan, Y., Papadaki, M. I. & Wang, Q. Life cycle assessment of metal–organic frameworks: sustainability study of zeolitic imidazolate framework-67. *ACS Sustain. Chem. Eng.* **11**, 4219–4225 (2023).
256. Dutta, S. et al. Cradle-to-gate environmental impact assessment of commercially available metal–organic frameworks manufacturing. *Adv. Funct. Mater.* **34**, 2410751 (2024).

Acknowledgements

The authors acknowledge the important contribution of the International Energy Agency (IEA) Hydrogen Technology Collaboration Programme (TCP) to this paper, specifically the activities of 'Task 40: Energy Storage and Conversion Based on Hydrogen'. The TCP is a unique global network that drives cutting-edge energy technology research through international cooperation. The authors also thank K. Hurst for discussions, L. Rochez-Ladeuze for help in preparing figures and K. Kisu for detailed verification of the descriptions regarding electrochemistry and batteries. M.B. acknowledges the support by Project CH4.0 under the Ministry of University and Research (MUR) programme 'Dipartimenti di Eccellenza 2023–2027' (CUP (Codice Unico di Progretto) D13C22003520001) and the project NODES, which received funding from the MUR and M4C2 1.5 of Piano Nazionale di Ripresa e Resilienza (PNRR) (grant ECS00000036). C.E.B. and T.D.H. acknowledge financial support from the Department of Industry, Science, Energy and Resources (2019 Global Innovation Linkage Grant GIL73589), the Australian Research Council (ARC) (Discovery Grant DP200102301, ARC Linkage Grants LP150100730 and LP190100297), the ARC Training Centre for The Global Hydrogen Economy (GlobH2E, IC200100023) and the Australian Renewable Energy Agency (ARENA) Materials for Transformative Research Accelerating Commercialisation (TRAC) Program (grant CB033). F.C. acknowledges funding from the Agence Nationale de la Recherche (ANR) through the H-BAT project (ANR-21-CE50-0030). M.D. acknowledges the support of the Leverhulme International Professorship Program (LIP-2021-018) of the Leverhulme Trust. S.D. and B.C.H. acknowledge support from the HYDROGENi Research Centre (hydrogeni.no), performed under the Norwegian research programme FMETEKN (Research Council of Norway, grant 333118). M.F. acknowledges financial support by the EFRE (Europäischer Fonds für regionale Entwicklung) Leitmarktwettbewerb Nordrhein-Westfalen EnergieUmweltwirtschaft within the project HyHeatStore (grant EFRE-0801550). D.M.G. acknowledges support from the UK Engineering and Physical Sciences Research Council (EPSRC) (grants EP/W005131/1 and EP/V042556/1). T.R.J. is grateful to the Independent Research Fund Denmark for Technology and Production (grant CaMBat DFF–0217-00327B). H.O. is grateful for partial funding by the National Research Foundation of Korea (grants 2022R1A2C3005978 and RS-2025-02982993). S-i.O. acknowledges the support of the JST Green Technologies of Excellence (GteX) Program Japan (grant JPMJGX23H1, MEXT/JSPS KAKENHI 'Hydrogenomics') and the Open Innovation Center of Hydrogen Science for GX (Green Transformation), Advanced Institute

for Materials Research (WPI-AIMR), Tohoku University. M.D.A., T.A., M.E.B. and B.C.W. gratefully acknowledge research support from the United States Department of Energy (DOE), Office of Energy Efficiency and Renewable Energy (EERE), Hydrogen and Fuel Cell Technologies Office through the Hydrogen Materials—Advanced Research Consortium (HyMARC). Additional support for B.C.W. was provided by the DOE EERE Vehicle Technologies Office. A portion of this work was performed under the auspices of the DOE by Lawrence Livermore National Laboratory under contract DE-AC52-07NA27344. Pacific Northwest National Laboratory is operated for the DOE by Battelle. Sandia National Laboratories is a multi-mission laboratory managed and operated by National Technology & Engineering Solutions of Sandia (NTESS), a wholly owned subsidiary of Honeywell International, for the DOE's National Nuclear Security Administration under contract DE-NA0003525. This written work is authored by an employee of NTESS. The employee, not NTESS, owns the right, title and interest in and to the written work and is responsible for its contents. Any subjective views or opinions that might be expressed in the written work do not necessarily represent the views of the United States Government. The publisher acknowledges that the United States Government retains a non-exclusive, paid-up, irrevocable, world-wide licence to publish or reproduce the published form of this written work or allow others to do so, for United States Government purposes.

Author contributions

All authors provided substantial contribution to discussion of content. All authors reviewed and edited the manuscript before submission.

Competing interests

D.P.B. is an employee of Hiden Isochema. Hiden Isochema is a manufacturer of hydrogen sorption instruments used to characterize hydrogen storage materials. The other authors declare no competing interests.

Additional information

Supplementary information The online version contains supplementary material available at https://doi.org/10.1038/s44359-026-00184-z.

Peer review information *Nature Reviews Clean Technology* thanks Jin-Yoo Suh, Kean Long Lim and Jianwei Ren for their contribution to the peer review of this work.

Publisher's note Springer Nature remains neutral with regard to jurisdictional claims in published maps and institutional affiliations.

[1]Hiden Isochema, Warrington, UK. [2]Sandia National Laboratories, Livermore, CA, USA. [3]Department of Chemistry, Washington University in St. Louis, St. Louis, MO, USA. [4]Pacific Northwest National Laboratory, Richland, WA, USA. [5]Department of Chemistry and NIS, University of Turin, Turin, Italy. [6]Institute of Hydrogen Technology, Helmholtz-Zentrum Hereon, Geesthacht, Germany. [7]Department of Physics and Astronomy, Curtin Institute for Energy Transition, Curtin University, Perth, Western Australia, Australia. [8]Dalian Institute of Chemical Physics, Chinese Academy of Sciences, Dalian, People's Republic of China. [9]Université Paris Est Creteil, CNRS, ICMPE, Thiais, France. [10]Institute for Energy Technology (IFE), Kjeller, Norway. [11]Department of Mechanical, Materials and Manufacturing Engineering, University of Nottingham, Nottingham, UK. [12]Max-Planck-Institut für Kohlenforschung, Mülheim an der Ruhr, Germany. [13]Université de Lorraine, Centre National de La Recherche Scientifique (CNRS), Institut Jean Lamour (IJL), Epinal, France. [14]Institute of Condensed Matter and Nanosciences, Université Catholique de Louvain, Louvain-la-Neuve, Belgium. [15]Hydrogen Research Institute, Université du Québec à Trois-Rivières, Trois-Rivières, Quebec, Canada. [16]Department of Chemistry, University of Hawaii Manoa, Honolulu, HI, USA. [17]iNANO and Department of Chemistry, Aarhus University, Aarhus, Denmark. [18]Materials Chemistry and Catalysis, Debye Institute for Nanomaterials Science, Utrecht University, Utrecht, The Netherlands. [19]Department of Chemistry, Ulsan National Institute of Science and Technology, Ulsan, Republic of Korea. [20]Advanced Institute for Materials Research (WPI-AIMR), Tohoku University, Sendai, Japan. [21]Institute for Materials Research, Tohoku University, Sendai, Japan. [22]Department of Physics and Astronomy, University of Bologna, Bologna, Italy. [23]National Institute of Advanced Industrial Science and Technology, Tsukuba, Ibaraki, Japan. [24]Department of Technology Systems (ITS), University of Oslo, Kjeller, Norway. [25]Hawaii Institute of Geophysics and Planetology (HIGP), University of Hawaii Manoa, Honolulu, HI, USA. [26]School of Environment and Science, Griffith University, Brisbane, Queensland, Australia. [27]Laboratory for Energy Applications for the Future (LEAF), Lawrence Livermore National Laboratory, Livermore, CA, USA. [28]Norwegian University of Science and Technology (NTNU), Trondheim, Norway. [29]School of Materials Science and Engineering, South China University of Technology, Guangzhou, China. [30]Max-Planck-Institut für Festkörperforschung, Stuttgart, Germany.